Chinese Journal of Natural Medicines

Advancements and applications in radiopharmaceutical therapy

Shiya Wang, Mingyi Cao, Yifei Chen, Jingjing Lin, Jiahao Li, Xinyu Wu, Zhiyue Dai, Yuhan Pan, Xiao Liu, Xian Liu, Liang-Ting Lin, Jianbing Wu, Ji Liu, Qifeng Zhong, Zhenwei Yuan

Citation: Shiya Wang, Mingyi Cao, Yifei Chen, Jingjing Lin, Jiahao Li, Xinyu Wu, Zhiyue Dai, Yuhan Pan, Xiao Liu, Xian Liu, Liang-Ting Lin, Jianbing Wu, Ji Liu, Qifeng Zhong, Zhenwei Yuan, Advancements and applications in radiopharmaceutical therapy, Chinese Journal of Natural Medicines, 2025, 23(6), 641-657. doi: 10.1016/S1875-5364(25)60887-9.

View online: https://doi.org/10.1016/S1875-5364(25)60887-9

Chinese Journal of Natural Medicines 23 (2025) 641-657

Contents lists available at ScienceDirect

Chinese Journal of Natural Medicines

journal homepage: www.cjnmcpu.com/

Review

Advancements and applications in radiopharmaceutical therapy

Shiya Wang[a,Δ], Mingyi Cao[a,Δ], Yifei Chen[a,Δ], Jingjing Lin[a], Jiahao Li[a], Xinyu Wu[a], Zhiyue Dai[a], Yuhan Pan[a], Xiao Liu[c], Xian Liu[b], Liang-Ting Lin[b], Jianbing Wu[a], Ji Liu[a,*], Qifeng Zhong[a,*], Zhenwei Yuan[a,*]

[a] *Department of Biomedical Engineering, School of Engineering, China Pharmaceutical University, Nanjing 210009, China*
[b] *Department of Health Technology and Informatics, The Hong Kong Polytechnic University, Hong Kong 999077, China*
[c] *School of Pharmacy and Jiangsu Province Key Laboratory for Inflammation and Molecular Drug Target, Nantong University, Nantong 226001, China*

ARTICLE INFO

Article history:
Received 9 October 2024
Revised 4 December 2024
Accepted 2 January 2025
Available online 20 June 2025

Keywords:
Radiopharmaceuticals
Radionuclide therapy
Alpha particle nuclide drugs
Beta particle radionuclide drugs
BNCT

ABSTRACT

Radiopharmaceuticals operate by combining radionuclides with carriers. The radiation energy emitted by radionuclides is utilized to selectively irradiate diseased tissues while minimizing damage to healthy tissues. In comparison to external beam radiation therapy, radionuclide drugs demonstrate research potential due to their biological targeting capabilities and reduced normal tissue toxicity. This article reviews the applications and research progress of radiopharmaceuticals in cancer treatment. Several key radionuclides are examined, including ^{223}Ra, ^{90}Y, Lutetium-177 (^{177}Lu), ^{212}Pb, and Actinium-225 (^{225}Ac). It also explores the current development trends of radiopharmaceuticals, encompassing the introduction of novel radionuclides, advancements in imaging technologies, integrated diagnosis and treatment approaches, and equipment-medication combinations. We review the progress in the development of new treatments, such as neutron capture therapy, proton therapy, and heavy ion therapy. Furthermore, we examine the challenges and breakthroughs associated with the clinical translation of radiopharmaceuticals and provide recommendations for the research and development of novel radionuclide drugs.

1. Introduction

In 1896, Henri Becquerel inadvertently discovered a novel type of ray capable of penetrating black paper and sensitizing photographic negatives. This discovery facilitated the scientific study of radioactive processes and identified the spontaneous penetrating rays emitted by uranium salts. This breakthrough revolutionized physics and laid the foundation for subsequent medical applications [1]. Becquerel's finding inspired the Curies to conduct extensive research on radioactive elements, leading to the discovery of polonium and radium, thereby paving the way for the utilization of radioactive materials in medicine [2]. In the early 20th century, George K. Heysham pioneered the use of radioactive ^{131}I for treating thyroid diseases [3], marking him as one of the early practitioners of radionuclide therapy (RNT). The advent of nuclear reactors, particle accelerators, and chemical separation technologies has significantly simplified and enhanced the acquisition of radioactive elements, greatly advancing the development of radiotherapy (Fig. 1)[4].

The initial form of radiopharmaceuticals was primarily salts, such as NaI, due to the thyroid's selective uptake of iodized salt. Phosphorus-32, in phosphate form, was utilized to treat certain blood disorders like polycythemia vera, owing to its uptake by rapidly dividing cells. However, direct salt administration presented limitations, including a lack of targeting and damage to non-target tissues. Radiopharmaceuticals have since evolved to incorporate chelates for binding radioactive elements, with targeted fragments attached. This development has expanded possibilities, reducing radioactive element release in the body, enhancing radionuclide stability, and extending drug action duration. The fundamental composition of modern radiopharmaceuticals comprises radionuclides, chelates, linkers, and targeting elements, including antibodies, peptides, small molecule fragments, and aptamers. Current clinical radiopharmaceutical chelating agents include 1,4,7,10-tetraazacyclododecane-1,4,7,10-tetraacetic acid (DOTA), which binds various trivalent metal radionuclides, and 1,4,7-triazacyclononane-1,4,7-triacetic acid (NOTA), suitable for binding divalent metals such as copper (Cu^{2+}). Contemporary research and development of radionuclides focus on two main areas: carrier innovation and targeted ligand innovation. This article will examine the application of emerging technologies such as nanoparticles (NPs), chelating agents, and polymers for nuclide drug carrier innovation, as well as the discovery of novel targets including peptides, small molecule probes, and bispecific antibodies [5].

In addition, *in vitro* treatment with radionuclides is also a component of radiation therapy. In the early 20th century, radium encapsulated in small metal containers was used for internal irradiation of cancerous tissue when inserted into the body. This

* Corresponding author.
E-mail addresses: jliu1618@163.com (J. Liu); zhong@cpu.edu.cn (Q. Zhong); yuanzhenwei@cpu.edu.cn (Z. Yuan)
Δ These authors contributed equally to this work.

https://doi.org/10.1016/S1875-5364(25)60887-9

early exploration of radioactive internal radiation therapy laid the foundation for the subsequent application of ^{90}Y microspheres. Extracorporeal irradiation therapy (EBRT) targets cancers from outside the body using high-energy rays or particles (such as protons, electron beams, X-rays, or heavy ions) to act directly on tumors [6, 7](Fig. 2). The radiation enters the tumor tissue and destroys it by rotating the equipment at a precise angle. Precise calculation of radiation field and dose is essential in the external beam radiation therapy treatment plan to enhance the likelihood of tumor control and minimize normal tissue damage [8]. Radiopharmaceuticals, conversely, represent a more precise treatment strategy. The advantage of radiopharmaceuticals lies in their high selectivity, enabling the delivery of therapeutic doses of radiation directly to the tumor site, thereby reducing damage to normal tissues [9-11]. This targeting also makes radiopharmaceuticals particularly suitable for treating metastasized tumors, as they can travel through the blood circulation to all parts of the body to treat metastases. Radionuclide drugs can be administered systemically [12, 13], orally or intravenously into the body, selectively concentrating at the lesion site. They can also be administered locally, such as by implanting radioactive particles or radioembolic microspheres [14, 15].

2. α particle nuclide drugs

Targeted alpha therapy (TAT) harnesses the distinctive characteristics of α particle radiation for cancer treatment. α particles are high-energy, high-charge particles with a short range (40–100 μm) and high linear energy transfer (LET = 80 keV/μm), rendering them highly suitable for precise localization and targeting of cancer cells [16]. This property enables effective and localized damage to tumor cells while minimizing the crossfire effect on surrounding healthy tissues, thus facilitating targeted delivery.

2.1. ^{223}Ra

^{223}Ra is a radioactive isotope of radium. It has a half-life of approximately 11.43 days. During its radioactive decay process, ^{223}Ra primarily undergoes α-decay, emitting α-particles (helium nuclei) and reducing the mass of its nucleus. This decay sequence ultimately results in the formation of ^{207}Pb.

In May 2013, the Food and Drug Administration (FDA) approved [^{223}Ra]$RaCl_2$, the world's first α-emitting radionuclide drug, for treating patients with castration-resistant prostate cancer (CRPC). [^{223}Ra]$RaCl_2$ has demonstrated efficacy against bone metastasis due to the chemical interchangeability of calcium and radium, particularly in areas of high bone turnover [17], which is highly selective for bone metastasis sites. The short-range α-radiation promotes localized cytotoxicity and anti-inflammatory effects by activating interleukin-2, contributing to its therapeutic impact [18].

Diniz Filho et al. [19] (Fig. 3) investigated the nanomechanical and ultrastructural effects of $^{223}RaCl_2$ on human breast cancer cells (lineage MDA-MB-231). The cells were cultured at drug doses of 2 μCi and 0.9 μCi. The researchers employed atomic force microscopy [20] (AFM) and transmission electron microscopy [21] (TEM) in conjunction with Raman spectroscopy to evaluate the effects. Their findings revealed significant disruption of the cell membrane, while the nuclear membrane remained intact [22].

Filippi et al. [23] investigated the relationship between overall survival (OS) and total lesion activity (TLA) in patients with metastatic CRPC [24] bone lesions treated with [^{223}Ra]$RaCl_2$ using positron emission tomography-computed tomography (PET-CT). Their findings indicate that a reduction in TLA following ^{223}Ra treatment may be associated with improved survival outcomes. In a separate study, Abbasi et al. [25] examined the dose distribution of $RaCl_2$ absorption in human organs. Their research revealed that the absorbed dose value of ^{223}Ra ($^{223}RaCl_2$) radiopharmaceutical in prostate organs was $9.47E^{-9}$ Gy/Bq. The biodynamic distribution of ^{223}Ra resulted in the highest absorbed dose in the thymus ($9.53E^{-8}$ Gy/Bq) and the lowest in the lens ($1.30E^{-10}$ Gy/Bq).

In the treatment of bone metastatic CRPC [26, 27], the gastrointestinal tract absorbs approximately 50% of the administered $^{223}RaCl_2$ dose, which limits uptake at the target site and potentially leads to toxicity. Abou et al. [28](Fig. 4) investigated the role of intestinal ion channels and their regulatory effects, revealing that amiloride (an epithelial sodium channel blocker) and NS-1619 (a K^+ channel activator) significantly influence $^{223}RaCl_2$ membrane transport. Amiloride redirected the uptake of $^{223}RaCl_2$ from the intestines and nearly doubled its accumulation at bone remodeling sites [17, 29]. The combination of these drugs demonstrated significantly enhanced inhibition of bone tumor growth compared to single-agent treatments, as measured by bioluminescence imaging and radiography. Notably, this combination therapy did not result in weight loss [30].

Rheumatoid arthritis (RA) is a chronic, inflammatory autoimmune disease [31, 32] that presents significant treatment challenges. Due to its prolonged nature, RA can result in severe musculoskeletal disorders, substantially impacting patients' quality of life [33, 34]. Correa et al. [35] investigated the use of low-dose [^{223}Ra]$RaCl_2$ (radium dichloride) as an intra-articular injection for

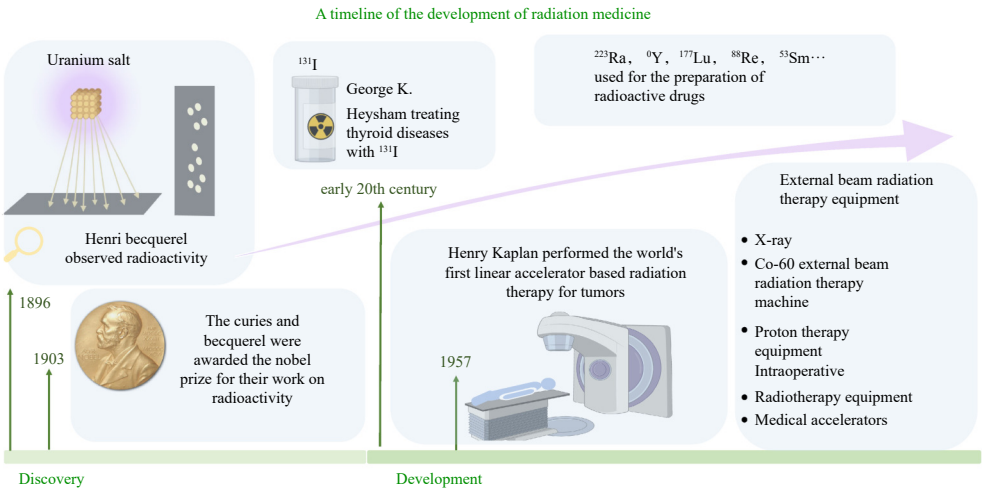

Fig. 1 A timeline of the development of radiation medicine.

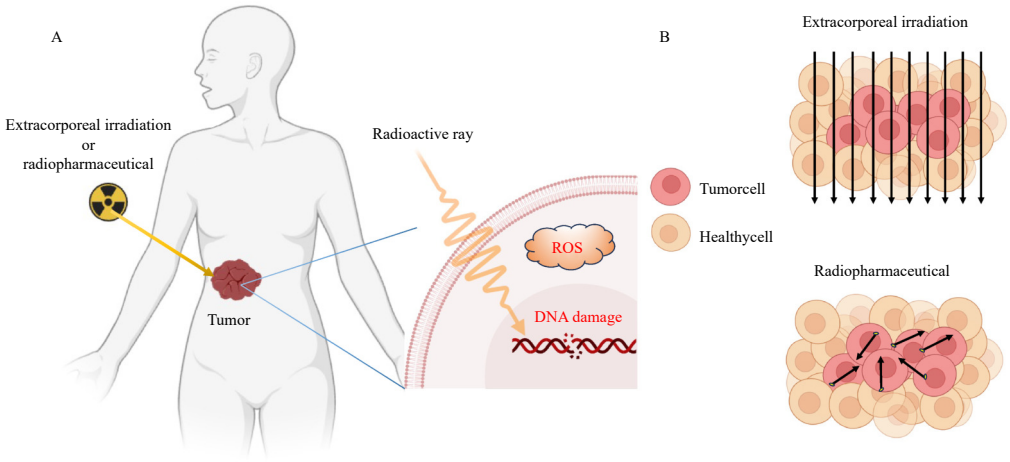

Fig. 2 (A) Principles of radiotherapy. (B) Difference between external beam radiation therapy and radiopharmaceutical therapy.

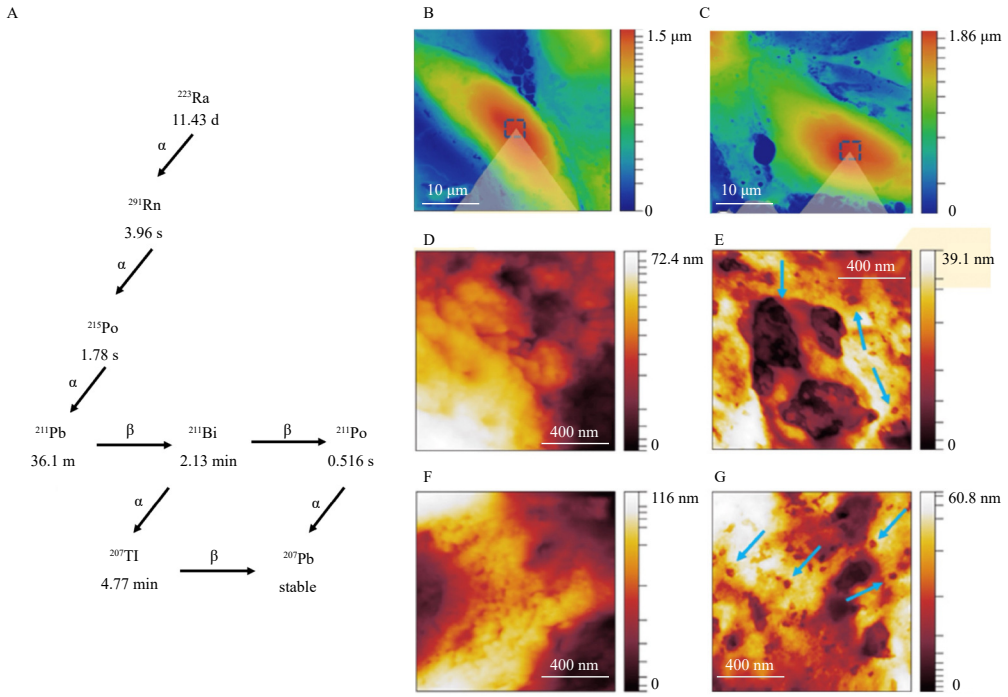

Fig. 3 (A) Schematic of ^{223}Ra decay. Atomic force microscopy (AFM) observed that cell damage. (B, D, F) was untreated and (C, E, G) treated by $^{223}RaCl_2$.

RA treatment. The study involved administering [^{223}Ra]$RaCl_2$ (1.48 μCi; i.a.) to mice 24 hours after zymosan stimulation. The results demonstrated that intra-articular injection of [^{223}Ra]$RaCl_2$ inhibited zymosan-induced artheroma-mediated leukocyte recruitment, with reductions of 69%, 77%, and 66% observed in total leukocytes, neutrophils, and monocytes, respectively.

The size of drug carriers significantly influences *in vivo* biodistribution, tissue penetration, and cellular uptake [36-38]. Consequently, when these vectors are loaded with therapeutic compounds, their dimensions can impact treatment efficacy. In internal α-RNT, the vehicle size is particularly crucial, as the short-range α-emitter must be delivered to the tumor volume at a high dose rate while minimizing side effects, such as off-target irradiation and toxicity.

Akhmetova et al. [39] (Fig. 5) investigated and contrasted calcium carbonate ($CaCO_3$) microparticles (MPs >2 μm) and NPs (< 100 nm) with radium-223 (^{223}Ra)-labeled internal α-radionuclides in treating 4T1 breast cancer. The researchers thoroughly examined the internalization and osmotic efficiency of these MPs and NPs using 2D and 3D cell cultures, revealing that ^{223}Ra-labeled NPs exhibited approximately 85% tumor suppression, surpassing 60% of ^{223}Ra-labeled MPs. Sakmar et al. [40] evaluated the outcomes of ^{211}Pb/^{211}Bi metabolites *in vivo* of ^{223}Ra surface-labeled TiO_2 NPs *in vitro* and ^{211}Pb in mouse models. The study noted that [^{223}Ra] can dissociate from its original carrier, migrate out of the target tissue, undergo translocation, and potentially accumulate in non-target organs.

2.2. ^{212}Pb

^{212}Pb can be derived from a ^{224}Ra generator. As a promising α-emitter, ^{212}Pb possesses an optimal half-life (10.6 h) and a favorable decay chain, making it a focal point of research in the field of RNT. Through its decay, ^{212}Pb produces α-particle emitters ^{212}Bi and ^{212}Po, thereby facilitating effective radiation treatment. Furthermore, ^{212}Pb functions as an *in vivo* generator of ^{212}Bi, effectively extending the latter's short half-life. When compared to ^{212}Bi for tumor targeting, ^{212}Pb offers a significant advantage: it delivers more than tenfold the dose per unit of administered activity. Additionally, its longer half-life enhances the practicality of dose

preparation and administration [41].

Banerjee et al. [42] developed a low molecular weight ligand for prostate-specific membrane antigen (PSMA) to assess its potential in targeted radiopharmaceutical therapy (RPT) for prostate cancer [43] by utilizing ^{203}Pb and ^{212}Pb radioisotopes. The study synthesized five low molecular weight ligands (L1-L5) using a lysine-urea-glutamate scaffold and determined their PSMA inhibition constants. While the Lutetium-177 (^{177}Lu)-PSMA-617 treatment group showed no survival benefit compared to the control group (median survival time of 46 and 47 days, respectively), the group administered ^{212}Pb-L2 (3.7 MBq) demonstrated a moderate but statistically significant improvement in median survival time (58 days, P = 0.002). These findings suggest that ^{212}Pb-labeled low-molecular-weight compounds may offer an effective treatment approach for prostate cancer, particularly for PSMA-positive tumors.

Li et al. [44] identified cluster of differentiation 46 (CD46) as a novel surface antigen of prostate cancer cells, demonstrating lineage-independent expression in both adenocarcinoma and small cell neuroendocrine subtypes of metastatic CRPC (mCRPC). The study revealed that the internalized human monoclonal antibody (mAb) YS5 can bind to tumor-selective CD46 epitopes. Consequently, ^{212}Pb, which generates α-emission ^{212}Bi and ^{212}Po *in vivo*, is conjugated to YS5 *via* the chelating agent TCMC to form the radioimmunoconjugated compound ^{212}Pb-TCMC-YS5.

Jiao et al. [45] utilized ^{203}Pb-labeled chimeric antibody targeting melanin c8C3 for micro single-photon emission computed tomography (SPECT)/CT imaging in mice with B16-F10 melanoma, while employing ^{212}Pb/^{212}Bi-labeled c8C3 for radioimmunotherapy (RIT). Their findings revealed that ^{212}Pb-c8C3 demonstrated dose-dependent efficacy within the 5–10 μCi range, inhibiting tumor growth and prolonging mouse survival. Kasten et al. [46] investigated the therapeutic potential of ^{212}Pb-labeled antibody 225.28, which targets chondroitin sulfate proteoglucan 4 (CSPG4), in TNBC mice. They observed a substantial accumulation of ^{212}Pb-225.28 in TNBC tumors [47], effectively extending mouse survival. While no significant dose-limiting toxicity was observed, treatment with ^{212}Pb-225.28 induced minor side ef-

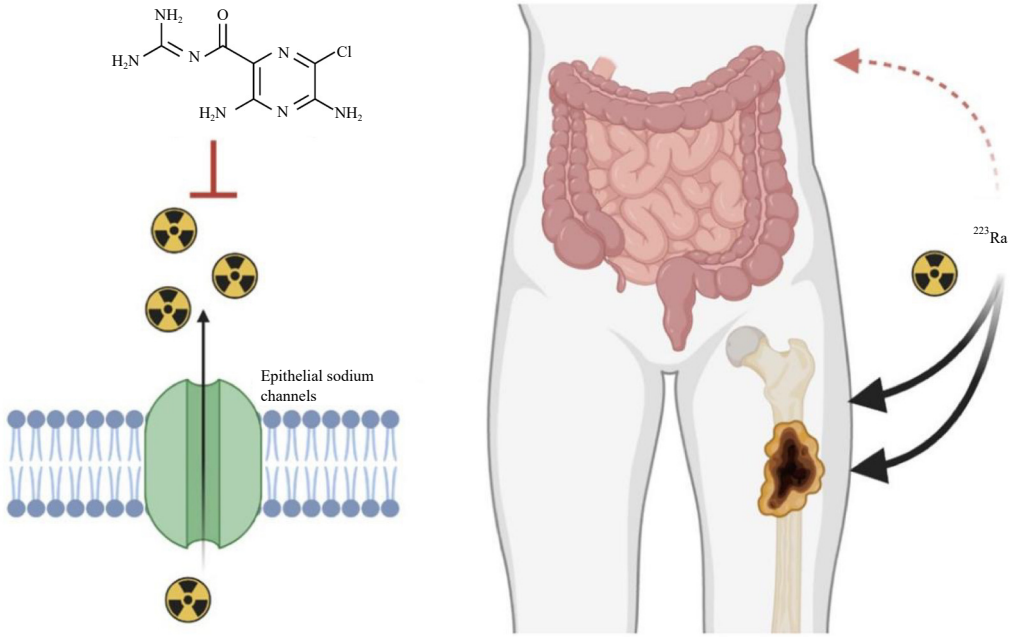

Fig. 4 Schematic of the effect of intestinal ion channels and their impact on the bone uptake of ^{223}RaCl$_2$.

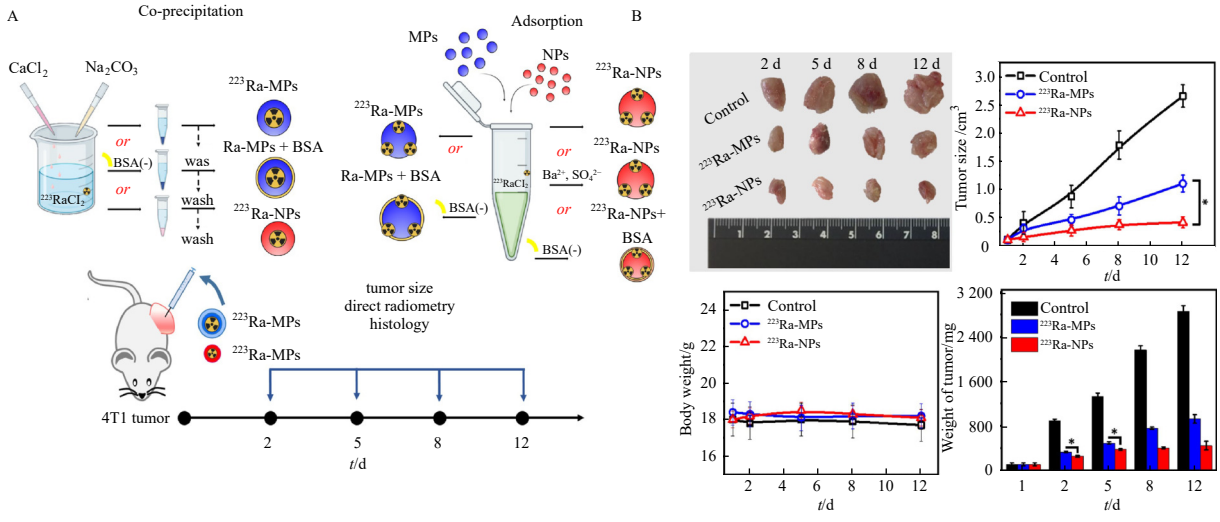

Fig. 5 (A) Radiolabeling of $CaCO_3$ MPs and NPs with ^{223}Ra. (B) Evaluation of the anti-tumor efficacy of $CaCO_3$ ^{223}Ra-MPs and ^{223}Ra-NPs intratumorally injected into 4T1 breast cancer-bearing mice.

fects, including nausea, hair loss, abdominal pain, diarrhea, and fatigue. These results suggest that ^{212}Pb-225.28 or its CSPG4-targeting radioimmunoconjugates (RICs) may be suitable for TNBC treatment, either as monotherapy or in combination with other approaches in future studies.

In conclusion, ^{212}Pb has demonstrated significant therapeutic efficacy across various cancer types, including prostate cancer, melanoma, endocrine tumors, and breast cancer. The ability to target ^{212}Pb to tumor cells through labeling with specific antibodies or peptides enhances its potential as a therapeutic agent. While clinical trials utilizing ^{212}Pb for RNT are still in their early stages, the considerable potential of this approach has garnered widespread attention. ^{212}Pb holds promise as a safe and effective novel modality for cancer treatment, potentially offering new hope for patients.

2.3. Actinium-225 (^{225}Ac)

^{225}Ac and ^{212}Pb are components of the ^{238}U-decay chain. ^{225}Ac is a promising α-emitting radionuclide for targeted radiotherapy of prostate cancer [48]. With a half-life of 9.92 days, ^{225}Ac's decay process involves six short-lived radioactive daughter nuclides, ultimately reaching a near-stable state of ^{209}Bi (half-life of approximately 19 trillion years) [49]. The decay of ^{225}Ac produces four net α particles, two β-emissions, and two gamma emissions, making it significant for therapeutic applications [50]. ^{225}Ac (α-particle emission, E_α is 5.8 MeV, $t_{1/2}$ 9.9 days) decays into ^{221}Fr (E_α 6.3 MeV, $t_{1/2}$ 4.8 min) and ^{217}At (E_α 7.1 MeV, $t_{1/2}$ 33 ms), followed by ^{213}Bi (E_α 5.8 MeV, 45.6 min). ^{213}Bi undergoes a branching decay (branching ratio 98%, E_β 1.4 MeV) to α-emitter ^{213}Po, and α-decay (2%, E_α 5.9 MeV) to ^{209}Tl. Both ^{213}Po (8.4 MeV, $t_{1/2}$ 3.7 μs) and ^{209}Tl decay to ^{209}Pb (E_β 1.4 MeV), followed by the stable ^{209}Bi. Two gamma radiations from the daughter ^{225}Ac ^{221}Fr (218 keV) and ^{213}Bi (440 keV) are utilized for imaging applications. Furthermore, α-particles' limited penetrability (short path length, 40–100 μm) enables effective targeted radiation delivery to local cancer cells while minimizing damage to surrounding healthy tissues, thus reducing off-target toxicity.

Compound ^{177}Lu-L1 [51] (Fig. 6) has demonstrated reduced off-target effects in prostate cancer xenograft models [52]. α-particle-emitting analogs of L1, specifically ^{213}Bi-L1 and ^{225}Ac-L1, were synthesized using this scaffold to assess their safety and cell-killing efficacy in PSMA-positive (+) xenograft models [53]. ^{225}Ac-L1 exhibits activity-dependent efficacy with minimal radiotoxicity to treatment-relevant organs. The development of superior bifunctional chelating ligands capable of sequestering both α-emitting radionuclides (^{225}Ac, ^{213}Bi) and their diagnostic counterparts (^{155}Tb, ^{111}In) remains a significant challenge in translating targeted α-therapy with complementary diagnostic imaging to clinical applications. To address this challenge, H(4)noneupaX, a chelating ligand featuring an unusual diametrically opposed arrangement of pendant donor groups, has been developed [54].

RNT necessitates a dose-based, personalized treatment strategy that relies on precise and consistent non-invasive measurements to ensure both safety and efficacy. While dose estimation using SPECT is feasible, it presents challenges for α-particle emitting RPT (α-RPT) due to complex gamma emission spectra, extremely low counts, and various image degradation artifacts across numerous scanner collimator configurations. The recently developed projection domain low-count quantitative SPECT (LC-QSPECT) method, which incorporates physics-based considerations and bypasses potentially lossy voxel-based reconstructions, shows promise in providing reproducible, accurate, and precise active concentration and dose measurements across multiple scanners, a common scenario in multicenter settings. Li et al. [55] conducted computed imaging experiments demonstrating that LC-QSPECT significantly enhanced reproducibility in terms of scanner-collimator configuration, accuracy, and retest repeatability compared to conventional reconstruction-based quantitation methods.

In summary, alpha particles demonstrate limited penetration (short path length: 40–100 μm), allowing precise radiation delivery to localized cancer cells with high efficiency while minimizing damage to adjacent healthy tissues, thus reducing off-target toxicity. The radioactive isotope ^{223}Ra exhibits notable therapeutic efficacy and an enhanced safety profile due to its minimal impact on surrounding healthy tissues; it shows strong selectivity towards bone metastases, promoting local cytotoxicity and anti-inflammatory effects. ^{212}Pb can selectively target tumor cells through specific antibody or peptide labeling techniques, offering advantages over ^{212}Bi, including delivering more than tenfold dosage per unit dosing activity due to its superior half-life, facilitating easier dosage preparation. ^{225}Ac-L1 demonstrates an activity-dependent effect with minimal radiotoxicity to treatment-related organs.

3. Beta particle radionuclide drugs

Despite the advantages of α-nuclides as radiopharmaceuticals in terms of radiolabeling chemistry, the number of α-therapeutic-nuclides is significantly lower than that of β-therapeutic-nuclides. β-decay is one of the most frequently utilized types of radionuclides in clinical RNT, characterized by the emission of β-particles (β^- or β^+, with β^+ often employed in PET imaging) or the process of capturing orbital electrons (EC decay). The energy transfer line density of β-rays typically remains below 1 keV·μm^{-1}, yet it demonstrates robust tissue penetration with a substantial radiation range of 1 to 11 millimeters. β-rays can directly target cells to induce single-strand deoxyribonucleic acid (DNA) breaks. Additionally, the efficacy of β-rays is enhanced by the bystander and cross-fire effects, which allow radiation to impact nearby cells and increase the overall effectiveness of RNT.

3.1. ^{90}Y

^{90}Y is a radioactive isotope of yttrium. It is characterized as a pure β-ray emitter. Typically, ^{90}Y is generated from ^{90}Sr, which is a byproduct of nuclear fission in reactors [56].

Hepatocellular carcinoma (HCC) represents the most common primary liver malignancy, contributing to 8% of cancer-related mortality. Transarterial chemoembolization (TACE) remains the standard treatment for patients with intermediate-stage (BCLC B) unresectable HCC and preserved hepatic function [57–59]. Transarterial radioembolization (TARE) is a localized RPT involving the administration of radioactive ^{90}Y microspheres to hepatic tumors (Fig. 7).

Costa et al. [61] demonstrated that the uEXPLORER scanner exhibited an improved signal-to-noise ratio compared to mCT, particularly in the low-count interstitial region, potentially enhancing dose quantification and tumor dosimetry. During the pre-treatment phase, (^{99m}Tc)-MAA SPECT-CT mock-up can assess dose delivery to tumors and normal liver, while post-treatment assessment utilizes ^{90}Y PET-CT acquisition. The optimal ^{90}Y activity for treatment was determined based on (^{99m}Tc)-MAA SPECT-CT dose results to effectively irradiate tumors while avoiding toxicity to healthy parenchyma. Richetta et al. [62] conducted a comparative dosimetry study using (^{99m}Tc) SPECT-CT and ^{90}Y PET-CT in 10 HCC patients. The Bland-Altman analysis revealed that variations in healthy parenchyma were lower than those in tumors (1.96 SD equals 9.1 Gy and 68 Gy, respectively), validating the robustness of the dose-toxicity approach. Post-treatment PET/CT imaging may indicate inadequate lesion dosing in ^{90}Y selective internal radiation therapy (SIRT) for HCC. Mee S F et al. [63] examined post-treatment PET/CT images of 20 HCC patients fol-

lowing ^{90}Y SIRT, suggesting that identifying HCC lesions or lesion subvolumes with insufficient SIRT administration could enhance tumor control and patient outcomes. This approach may also enable SIRT to serve as a targeted debulking tool when stereotactic body radiation therapy (SBRT) is not independently feasible.

The integration of molecular and external radiotherapy presents a promising therapeutic approach, potentially enhancing localized tumor dosage while minimizing damage to surrounding healthy tissues. Dietrich et al. [64] investigated the combination of a ^{90}Y-labeled anti-epidermal growth factor receptor (EGFR) antibody (Cetuximab) with clinically relevant fractionated radiotherapy in a preclinical study using xenograft tumors in head and neck squamous cell carcinoma. The results demonstrated significantly improved tumor growth control in the combination therapy compared to radiotherapy alone. This study suggests that radiolabeled therapy, when combined with clinically relevant fractionated radiotherapy, holds substantial potential for improving curative treatment outcomes.

Pyclen-dipicolinate chelates have demonstrated exceptional efficacy as chelating agents for radiolabeling with β-emitters, particularly ^{90}Y. Le et al. developed pyclen-dipicolinate ligands with additional C12-alkyl chain functionalization. Their research revealed that the incorporation of saturated carbon chains did not compromise the radiolabeling efficiency with ^{90}Y, while significantly enhancing the lipophilicity of the resulting radiocomplexes. This characteristic enables the compound's extraction in lipiodol and encapsulation in biodegradable pegylated polymalate NPs [65, 66]. These findings underscore the potential of lipophilic xadiene-dipyridinylcarboxylate derivatives as a foundation for developing radiopharmaceuticals targeted at liver or brain cancer treatment through in-house radiotherapy.

Winter's modification [67] of CD66b-specific mAbs using DTPA-based chelating agents is anticipated to improve the absorbed dose distribution during therapy. Furthermore, hematopoietic cell transplantation (HCT) demonstrates good tolerability following pretreatment with radioactive anti-neutrophil therapy (RANT). These encouraging preliminary results suggest that further investigation into the adjuvant opsonization of ^{90}Y-DTPA-BN-CHX-A-anti-CD66-mAb in HCT is merited.

^{90}Y dosimetry studies present challenges due to the lack of precise and accurate methods. However, combining PET with Monte Carlo simulations and other imaging modalities is considered optimal for calculating segmented dose distributions. Budzynska et al. [68] assessed the accuracy of LSF estimation through phantom imaging and analyzed high-activity ^{90}Y post-processing scans and ^{90}Y activity of approximately 100 MBq pre-processing hybrid imaging techniques using various nuclear imaging methods. Unlike ^{99m}Tc, ^{90}Y does not emit specific nuclear gamma radiation. Imaging relies entirely on bremsstrahlung radiation generated by decelerating β-particles, and PET/CT can accurately estimate LSF during treatment following ^{90}Y administration. However, at lower activities around 100 MBq, it appears to provide unreliable estimates. PET imaging facilitates improved visualization of both hot and cold tumors.

3.2. ^{177}Lu

^{177}Lu demonstrates significant potential in clinical applications and is increasingly replacing ^{90}Y-labeled peptides in receptor-targeted therapies. As a lanthanide with atomic number 71, ^{177}Lu undergoes β-decay, emitting β-particles with an average energy of 0.497 MeV. Its half-life of approximately 6.65 days and tissue path length (average 0.16 mm, maximum 2 mm) make it ideal for treating disseminated metastatic cancers while minimizing damage to normal tissues. The therapeutic β-particle emission of ^{177}Lu is accompanied by γ photons of 208 keV (10.4%) and 113 keV (6.2%) [69]. The physical half-life ($t_{1/2}$ = 6.64 d) of ^{177}Lu facilitates its supply, logistics, and clinical application across a wide range of targeted agents, from peptides to large biomolecules, rendering it highly suitable for radiopharmaceutical treatment and dosimetry purposes.

^{177}Lu, formed by binding to a high-affinity somatostatin analog (octrastyic acid) *via* a DOTA chelator molecule, was approved by the FDA in 2018 as ^{177}Lu-DOTATATE therapy for the treat-

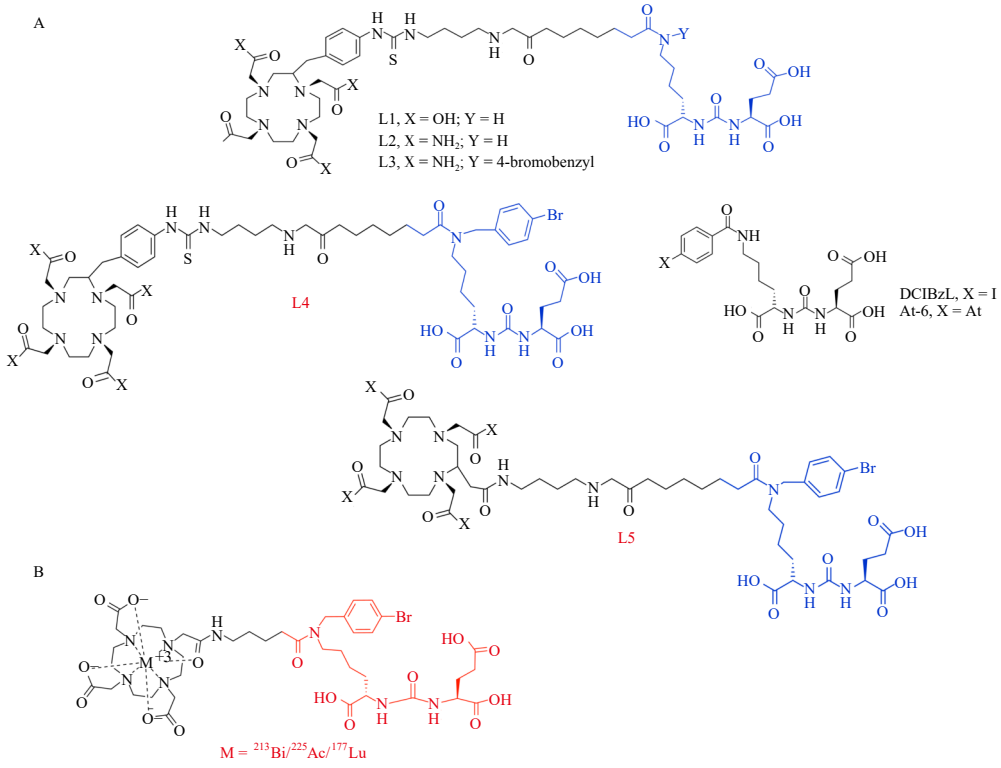

Fig. 6 (A) Structures of DCIBzL, 211At-6, and ligands L1–L5, for 203/212Pb-labeled PSMA-targeted α-particle theranostics. (B) Chemical structures of ^{213}Bi-L1 and ^{225}Ac-L1.

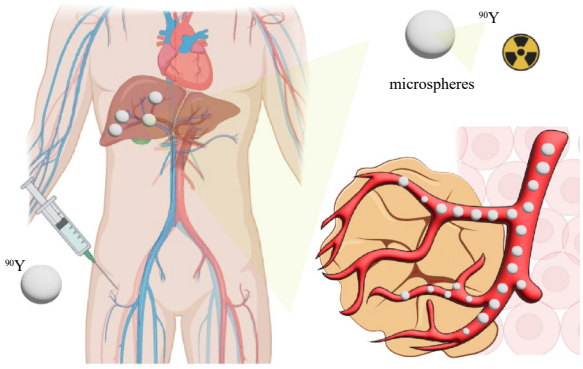

Fig. 7 Schematic of ^{90}Y microsphere treatment [60].

ment of somatostatin receptor (SSTR)-positive gastroenteropancreatic neuroendocrine tumors [70-72]. [^{177}Lu]Ludotadipep, a novel prostate-specific membrane antigen-targeting therapy, incorporates albumin motifs to enhance tumor uptake. This treatment is anticipated to be safe at a dose of 3.7 GBq administered over 6 cycles, with kidneys and bone marrow identified as key organs at risk (OARs). [^{177}Lu] Ludotadipep has demonstrated a high tumor-absorbed dose and is scheduled for evaluation in a phase II clinical trial [73].

Banerjee et al. [74] (Fig. 8) developed and evaluated 14 novel PSMA-targeted ^{177}Lu-labeled radioligands (^{177}Lu-L1-^{177}Lu-L14) utilizing various chelators and linkers. Their assessment included *in vitro* studies using human prostate cancer PSMA-positive (PC3 PIP) and PSMA-negative (PC3 flu) cell lines, as well as corresponding flank tumor models. The efficacy and toxicity of ^{177}Lu-L1, ^{177}Lu-L3, ^{177}Lu-L5, and ^{177}Lu-PSMA-617 were evaluated over an 8-week period using a single 111 MBq dose. Further investigations examined the efficacy of ^{177}Lu-L1 at different doses and assessed long-term toxicity in healthy immunocompetent mice. The radioligands demonstrated high radiochemical yields and purity. Cellular uptake and internalization studies [75] revealed specific uptake exclusively in PSMA-positive PC3 cells.

Liposomes represent promising drug delivery systems due to the reduced toxicity of liposome-encapsulated drugs. However, broader clinical applications necessitate more effective tumor-targeting [76-78], including enhanced uptake, controlled drug release, and extended shelf life. Cvjetinovic et al. [79] (Fig. 9) exploit the unique metabolic properties of cancer cells, specifically their higher energy requirements and increased glucose utilization, in the design of glucose-modified liposomes (GMLs). This approach aims to provide improved tumor targeting and increased drug delivery to tumor cells *via* glucose transporters. Utilizing ^{177}Lu as a radiomarker, a straightforward and reliable radiotracer method demonstrated the tumor accumulation potential of GML in CT26 and LS174T tumor-bearing mice.

Generally, radioactive β particle-emitting drugs demonstrate robust tissue penetration and a substantial radiation range (1−11 mm), enabling direct cellular targeting to induce DNA single-strand breaks. Moreover, they can affect adjacent cells through crossfire and bystander effects, thereby enhancing radioisotope therapy efficacy. These agents not only facilitate controlled drug release but also exhibit extended shelf life and superior tumor-targeting specificity.

4. Proton/heavy ion therapy and boron-neutron capture therapy

Conventional radiotherapy utilizes photon-based radiation, such as X-rays and gamma rays, while proton therapy is classified as a form of particle therapy. Proton therapy exploits the Bragg peak phenomenon (Fig 10A), wherein high-velocity particles release a substantial amount of energy immediately before coming to rest. In this treatment modality, particles are accelerated to approximately 0.7 times the speed of light and then precisely directed into the patient's body [80]. Upon reaching the cancer cells, these particles release a significant amount of energy, effectively destroying the malignant cells.

The field of proton and heavy ion radiotherapy for tumor treatment has experienced rapid advancement in recent years. According to the Particle Therapy Co-Operative Group (PTCOG), as of December 2014, 48 proton and heavy ion therapy centers were operational worldwide, collectively treating 137 179 patients. This therapeutic approach capitalizes on the physical properties of protons and heavy ions as they traverse matter, creating a Bragg peak (Fig. 10A). The dose distribution in proton and heavy ion radiotherapy demonstrates superior characteristics compared to photon radiotherapy, enabling increased tumor therapy doses while minimizing damage to normal tissue. Current research extensively explores the efficacy and safety of proton and heavy ion therapy for various malignancies, including head and neck tumors, lung cancer, esophageal cancer, and liver cancer.

4.1. Proton radiation therapy (PRT)

Leptomeningeal metastasis (LM) represents a severe complication of advanced malignancies with a poor prognosis. Untreated LM patients have a median survival of only 2-4 months [82, 83]. Currently, photon involved-field radiotherapy (IFRT) is frequently employed for LM treatment. However, IFRT proves ineffective in preventing disease progression when tumor cells are widely disseminated throughout the central nervous system. In contrast to conventional photon therapy, proton therapy offers potential benefits for LM patients due to its characteristic Bragg peaks. Barney et al. [84] conducted a retrospective analysis of 50 consecutive patients (aged 16-63 years) with diverse histological malignancies who underwent vertebral body-preserving proton craniospinal irradiation (p-CSI) treatment at MD Anderson Cancer Center from 2007 to 2011. The study assessed acute toxicity and preliminary clinical outcomes in adults receiving p-CSI treatment. The findings indicated that proton therapy can mitigate the associated toxic side effects in the treatment of advanced brain metastases compared to photon therapy. Adeberg et al. [85] classified patients with intracranial tumors undergoing PRT based on tumor location. They subsequently replanned the treatments using three-dimensional conformal radiotherapy (3DCRT) and intensity-modulated radiotherapy (IMRT) to evaluate the dose reduction to multiple OARs with PRT for various tumor sites. The study demonstrated that PRT offers superior protection to critical organs compared to 3DCRT and volumetric modulated arc therapy (VMAT), particularly reducing the risk of damage to the temporal lobe and hippocampus associated with memory impairment [86, 87].

Yang et al. [88] conducted a phase I B clinical study to assess the effectiveness of p-CSI for brain metastases. The study revealed that patients treated with p-CSI experienced a decrease in average cerebrospinal fluid-circulating tumor cells (CSF-CTCs), whereas those treated with IFRT showed an increase in average CTC count. These findings suggest that proton therapy for LM may reduce CSF-CTCs and potentially improve patient survival rates.

A patient diagnosed with medulloblastoma [89] underwent p-CSI utilizing a bone marrow-sparing technique. This approach minimized radiation exposure to structures anterior to the vertebrae while administering the full prescribed dose to the spinal canal. Magnetic resonance imaging (MRI) scans revealed fatty bone marrow replacement in the vertebral bodies, consistent with the treatment's dose distribution. CT images corroborated

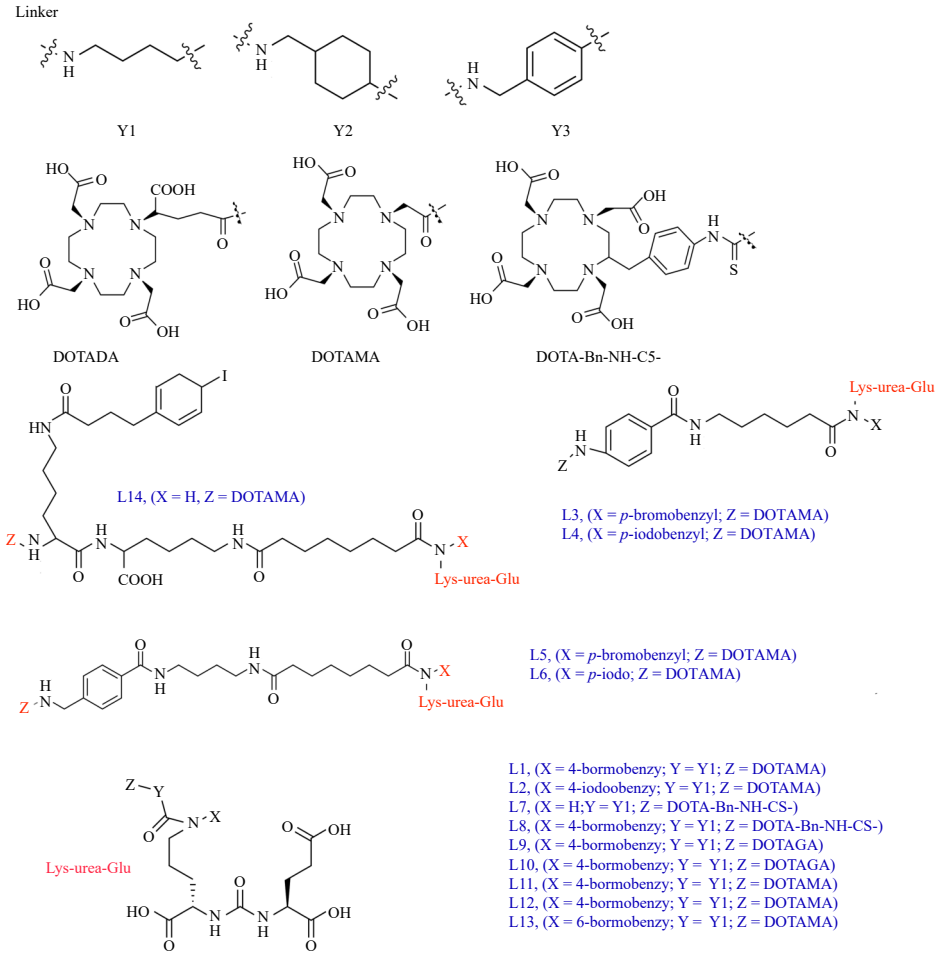

Fig. 8 ^{177}Lu-labeled radioligands with chelators (^{177}Lu-L1-^{177}Lu-L14).

the treatment plan, including the boost phase [90].

In comparison to photon therapy, PRT for lung cancer demonstrates the ability to minimize radiation exposure to surrounding healthy tissues and organs, including the lungs, heart, and spinal cord. This advantage enables potential dose escalation to the target while maintaining tolerability when combined with other treatment modalities, such as chemotherapy. PRT may offer enhanced safety for recurrent tumors [91, 92]. Currently, PRT exhibits promising potential in treating inoperable or ineligible patients with stage I non-small cell lung cancer (NSCLC) and locally advanced NSCLC. These applications are particularly relevant given the inherent limitations of the disease itself [93-95].

The dosimetric advantage of PRT is particularly significant for pediatric tumor patients. Previous studies have demonstrated that PRT can substantially reduce the average dose to critical structures such as the hippocampal gyrus, dentate gyrus, subependymal area, supratentorial and infratentorial brain, temporal lobe, pituitary, and optic chiasm. Furthermore, PRT has shown the potential to improve local control rates and survival rates in osteosarcoma and prostate cancer cases, while reducing adverse effects on surrounding tissues [96, 97]. PRT also exhibits promising therapeutic effects for gastrointestinal tumors. However, the dose distribution in PRT is significantly influenced by postural changes and respiratory motion, presenting challenges in treatment planning and execution. Due to the rapid dose attenuation outside the target area in PRT, accurate target delineation is crucial in the era of "involved field" radiotherapy. Nonetheless, the high cost of PRT necessitates careful consideration by radiation oncologists to weigh the technological advantages against the expenses and select patients who are most likely to benefit from this treatment modality.

4.2. Heavy ion radiotherapy

Heavy ion radiotherapy demonstrates a potent tumor-killing effect by inducing double-strand DNA breaks in cancer cells, rendering them irreparable and ultimately achieving complete eradication of the cancerous cells. The cytotoxic capacity of heavy ions is 2 to 3 times greater than that of conventional X-ray radiotherapy. Heavy ions possess both physical and biological advantages and show broad prospects for development. Carbon ions are the most frequently utilized heavy ions in treatment. Carbon ion therapy has demonstrated efficacy against radiation-resistant head and neck tumors such as mucosal malignant melanoma and adenoid cystic carcinoma. Peripheral stage I NSCLC requires only four sessions, with survival rates comparable to the best photon SBRT outcomes. Furthermore, for inoperable sacral chordomas, carbon ion therapy achieves a five-year local control rate of 88% and a survival rate of 86%, although sciatic nerve injury occurs in 15% of patients. In a study involving 69 patients with primary liver cancer treated with carbon ion therapy, no treatment-related liver injury was observed, with a five-year local control rate of 81% and a survival rate of 33% [98–100]. For unresectable locally advanced pancreatic cancer treated with carbon ion therapy and gemcitabine chemotherapy, the two-year local control rate was 58%, and the overall survival rate was 54%, surpassing the outcomes of photon IMRT [101]. Additionally, Combs et al. [102] report that carbon ion radiotherapy for brain and skull base tumors has demonstrated potential to reduce the incidence of secondary malignancies and enhance patient quality of life. Nonetheless, these preliminary findings necessitate confirmation through long-term follow-up studies to establish their sustained efficacy and clinical relevance.

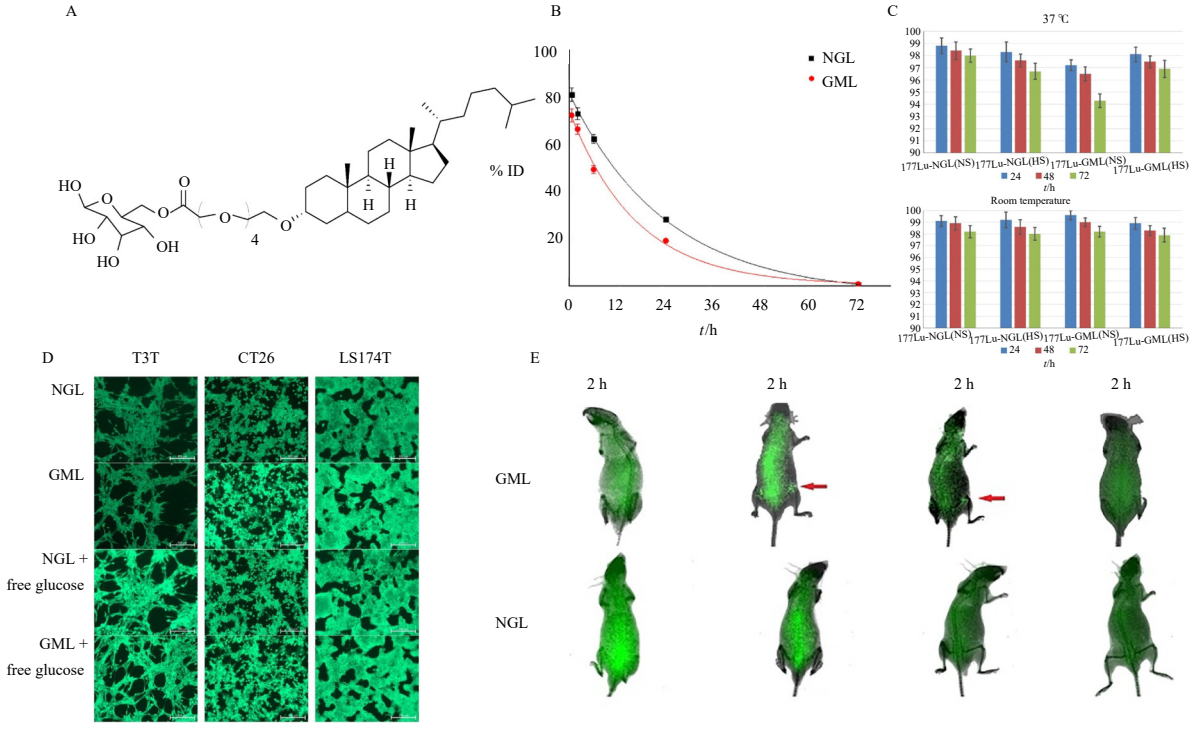

Fig. 9 Glucose-modified liposomes (GMLs) increased the drug delivery to tumor cells. (A) Structural of Glycosyl derivative of cholesterol-L. (B) Blood clearance profile of ^{177}Lu-NGL and ^{177}Lu-GML. (C)Fluorescence microscopy images of NGL/GML in different cells (10 min incubation). (D)Imaging studies on LS174T tumor-bearing NOD/SCID mice after intravenous injection of ^{177}Lu-GML and ^{177}Lu-NGL (red arrows indicate the position of LS174T cancer sites). (E)Imaging studies on LS174T tumor-bearing NOD/SCID mice after intravenous injection of 177Lu-GML and 177Lu-NGL (red arrows indicate the position of LS174T cancer sites).

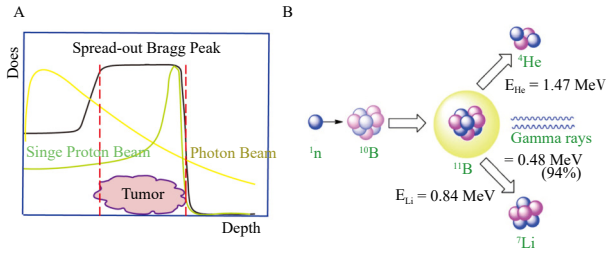

Fig. 10 Proton therapy, heavy ion therapy, and boron neutron capture therapy represent more precise forms of radiotherapy. (A) Bragg Peak Diagram. (B) Principles of Boron Neutron Capture Therapy [81].

In conclusion, proton and heavy ion therapies offer superior tumor dose distribution, enabling increased tumor dosage while minimizing damage to normal tissues. Heavy ion therapy, in particular, demonstrates enhanced biological effectiveness, making it advantageous for treating tumors resistant to conventional photon radiation. Currently, multiple clinical studies are underway comparing photon and proton therapies for various tumors, with a phase III clinical trial for heavy ion therapy in preparation. The results of these studies will provide valuable insights into the characteristics and advantages of proton and heavy ion therapies, facilitating more accurate patient selection and promoting the rational application of these advanced radiotherapy techniques.

4.3. Boron neutron capture therapy (BNCT)

BNCT represents an innovative, non-invasive approach to treating solid tumors, including brain cancer, head and neck cancer, and melanoma. The fundamental principle of BNCT involves a nuclear reaction between a non-toxic thermal neutron beam and ^{10}B atoms. This reaction generates alpha particles and ^{7}Li, which possess the capability to disrupt DNA bonds in individual cells containing ^{10}B atoms (Fig. 11) [103]. As a targeted biochemical radiotherapy, BNCT demonstrates enhanced precision and safety compared to conventional chemotherapy and radiotherapy methods [104].

An effective boron carrier must meet several essential criteria [106]: (1) It should facilitate high absorption of ^{10}B atoms by tumor cells or tissues, with concentrations exceeding 20 μg per gram of tumor tissue; (2) Boron atoms should accumulate preferentially in tumor cells, with a tumor-to-blood (T/B) or tumor-to-

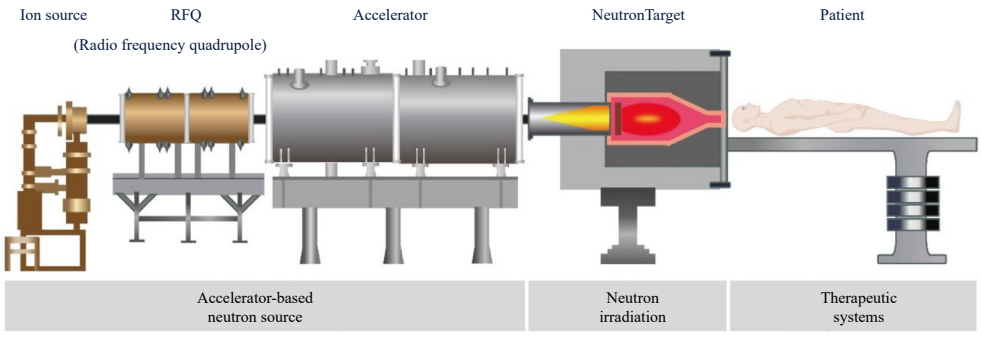

Fig. 11 Schematic diagram of accelerator-based BNCT configuration[105].

normal tissue (T/N) concentration ratio greater than 3 : 1; (3) The carrier must demonstrate low cytotoxicity. Currently, two compounds are clinically employed in BNCT: Boron phenylalanine (BPA) and sodium borate n-butyrate (BSH). BPA selectively enters tumor cells due to its high affinity for L-amino acid transporter 1 (LAT1), which is overexpressed in various tumors to support their nutritional requirements for growth and proliferation [107]. However, BPA has limitations including low boron content and susceptibility to direct hydrolysis into boric acid. Conversely, BSH exhibits low cytotoxicity but lacks tumor-targeting ability and deep permeability into hypoxic zones within tumors, restricting its further application in solid tumor treatment [108].

To overcome the limitations of BPA and BSH, researchers have developed various boron-containing drugs and drug delivery systems. However, these approaches primarily focus on enhancing boron concentration at the tumor site without adequately considering the microenvironment or heterogeneity of solid tumors. Consequently, the development of new boron-containing drugs should prioritize both high boron content and tumor specificity.

Addressing the need for optimal BNCT preparations that meet specific requirements while delivering high boron concentrations to tumor sites with sustained retention during neutron irradiation therapy, Yuan et al. [109] (Fig. 12) developed a series of non-toxic dual-targeting boron carriers. The carriers B139, B142, and B151 selectively interact with LAT1 and exhibit affinity for hypoxic tumor microenvironments, enabling preferential accumulation within malignant cells. These agents demonstrate markedly higher uptake in hypoxic tumor regions relative to conventional compounds such as BPA. *In vivo* studies demonstrated prolonged retention at therapeutic concentrations, reaching a peak of 50.7 μg·kg^{-1} with a T/B ratio exceeding 3, suggesting their potential as ideal candidates for BNCT applications.

The successful clinical implementation of BNCT relies on interdisciplinary collaboration and advancements in various fields, including nanotechnology, to facilitate its development. Although challenges persist, BNCT has demonstrated superior outcomes in prolonging survival rates and minimizing side effects compared to conventional treatment modalities.

Consequently, interdisciplinary collaboration among researchers is essential to optimize the clinical efficacy of BNCT. The development of next-generation boron-containing compounds with enhanced tumor-targeting properties and reduced adverse effects represents a promising avenue for future BNCT research. Ongoing investigation of diverse targeting approaches will contribute to the eventual clinical implementation and widespread accessibility of BNCT as a therapeutic option for cancer patients.

5. Research progress of radionuclide medicine and imaging

Photodynamic therapy (PDT) is extensively utilized in clinical research and practice for tumor treatment, owing to its high selectivity and minimal invasiveness [110-112]. Nevertheless, conventional PDT is typically restricted to superficial tissues due to the limited penetration depth of visible light. During radioactive decay, nuclei can emit ultraviolet to blue visible light, a phenomenon known as Cherenkov radiation (CR), when charged particles exceed the speed of light in the medium [113]. Radioactive nuclei and CR can serve as internal excitation sources to activate photosensitizers for deep-tissue PDT. However, the therapeutic efficacy of CR is constrained by its low efficiency [114].

To enhance the therapeutic effect for deep-seated tumors, Sun et al. [115]developed a ^{131}I-labeled tetrakis (4-carboxyphenoxy) phthalocyaninatozinc (II) ($ZnPcC_4$) conjugated Cr^{3+} doped gallium zinc oxide ($ZnGa_2O_4 : Cr^{3+}$, ZGCs) nanoplatform for combined RT and radiation-induced PDT. ZGCs are luminescent NPs that exhibit continuous emission in the near-infrared region (NIR), driven by a broad excitation spectrum spanning from ultraviolet to visible wavelengths [116, 117]. ^{131}I exerts a dual therapeutic function by triggering ZGCs through CL and ionizing radiation, resulting in sustained near-infrared emission that subsequently activates the photosensitizer ZnPcC4 for PDT. In parallel, ^{131}I directly induces cytotoxicity in cancer cells. The ^{131}I-ZGCs-ZnPcC4 demonstrated effective tumor suppression both *in vitro* and *in vivo*. By combining self-activated PDT and RT, ^{131}I-ZGCs-ZnPcC4 significantly enhances the treatment of deep-seated tumors. CR activation of a photosensitizer addresses the issue of limited light penetration in conventional PDT [118, 119]. However, the injection of radioactive drugs and PS alone does not guarantee their effective interaction in the tumor region [120], and the simultaneous delivery of radioactive nuclides and PS in normal tissue presents a considerable phototoxicity problem.

In 2021, Sun et al. [121] developed an innovative ^{131}I-labeled photosensitizer. This compound comprises phospho-a (photosensitizer), diisopropyl (pH-sensitive group) [122], ^{131}I-labeled tyrosine (CR donor), and polyethylene glycol, which self-assemble into NPs (^{131}I-sPS NPs) [123]. These ^{131}I-sPS NPs exhibit reduced phototoxicity in normal tissue due to an aggregation-induced quenching effect, while still generating active oxygen at tumor sites post-decomposition. Following intravenous administration, ^{131}I-sPS NPs demonstrated significant anti-tumor efficacy in both 4T1 tumor-bearing Balb/c mice and *in situ* VX2 tumor-bearing rabbits. This research suggests that ^{131}I-sPS NPs may broaden the applica-

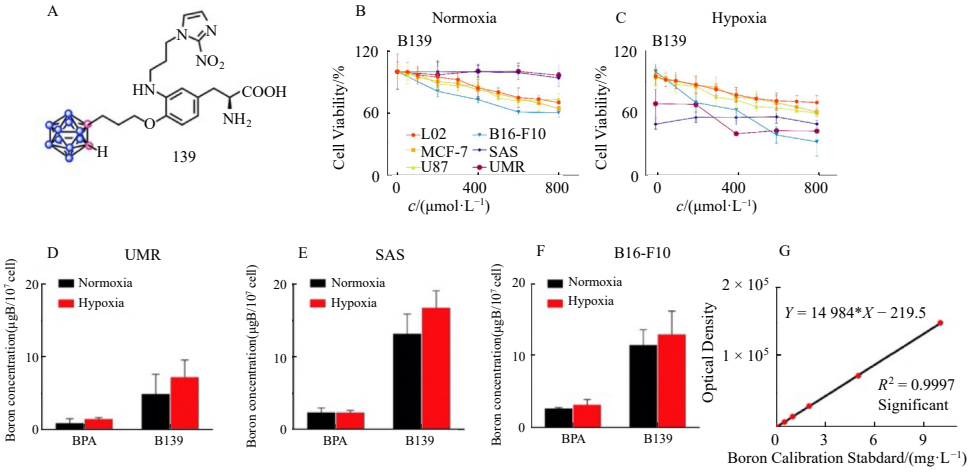

Fig. 12 (A) Boron-containing target molecule. (B–C) Effect of B139 on the viability of normoxia and hypoxic cells *in vitro* within 24 h of co-incubation. (D–G) Cellular uptake of B139 and BPA under normoxia and hypoxia UMR, SAS, and B16-F10 cells *in vitro*.

tion scope of CR and offer effective strategies for treating deep-seated tumors.

Cherenkov radiation-induced photodynamic therapy (CR-PDT) addresses the light penetration limitations of conventional PDT [124]. However, the concurrent circulation of radioactive nuclides and photosensitizers may induce persistent phototoxicity in healthy tissues. 5-Aminolevulinic acid (ALA), a cancer-selective photosensitizer, converts intracellularly into the photosensitizer protoporphyrin IX (PpIX) with minimal side effects. Nevertheless, the therapeutic efficacy of ALA-based PDT is considerably impeded by ALA's hydrophilic nature and the subsequent transformation of PpIX into photosensitive heme.

In 2023, Sun et al. [124] developed an ^{89}Zr-labeled, pH-responsive ALA and artemisinin (ART) co-loaded liposome (^{89}Zr-ALA-Liposome-ART) for highly selective cancer therapy. ^{89}Zr functions as an internal excitation source to activate PpIX for CR-PDT [110, 111], while the photo-inactivated Heme activates the chemotherapeutic effect of ART. Through CR-PDT and chemotherapy, ^{89}Zr-ALA-Liposomes-ART demonstrated effective tumor suppression in subcutaneous 4T1 tumor-bearing Balb/c mice. When combined with anti-PD-L1, ^{89}Zr-ALA-Liposomes-ART induced enhanced anti-tumor immunity and inhibited tumor recurrence.

Chemotherapy, utilizing cytotoxic drugs to eradicate tumors, remains a primary cancer treatment modality [125]. However, this approach is hindered by limitations such as insufficient tumor specificity and unintended toxicity to healthy tissues [126]. PDT [118], which employs light to modulate drug activity, offers a non-invasive and spatiotemporally controlled method to manage chemotherapeutic effects [127]. While radioactive drug therapy using radiolabeled tracers is well-established, the application of radioactive isotopes in PDT for reversible regulation of drug biological effects remains largely unexplored.

Sun et al. [128] (Fig. 13A) recently employed PDT to incorporate azoPROTAC, a class of photochromic switches, into drugs, enabling light-mediated control of pharmacological activity in space and time. Their research demonstrated that ^{131}I could induce trans-photoisomerization of azoPROTAC-containing PROTACs. Under the influence of 50 μCi mL^{-1} ^{131}I, the azoPROTAC effectively reduced the levels of BRD4 and c-Myc in 4T1 cells, achieving results comparable to those observed under illumination (405 nm, 60 mW cm^{-2}).

Furthermore, the degradation of BRD4 could enhance the efficacy of ^{131}I-based radiotherapy. *In vivo* studies demonstrated that the combination of 300 μCi ^{131}I and 25 mg·kg^{-1} azoPROTC, administered *via* a hydrogel, successfully induced protein degradation *in vivo* in 4T1 tumor-bearing mice. This approach effectively inhibited tumor growth, augmented the radiotherapeutic effect, and enhanced the anti-tumor immune response. Notably, this represents the first successful application of radioactive isotopes as a PDT trigger in a murine model [129]. This research is expected to contribute significantly to the advancement of deep-tissue PDT [130].

Colorectal cancer (CRC) [131-133] ranks as the third most prevalent malignancy worldwide, with early detection significantly improving prognosis. The gastrin-releasing peptide receptor (GRPR) exhibits high expression levels in CRC cells, rendering it a potential biomarker for CRC diagnosis [134]. Bombesin (BBN) peptide analogs [135] have been extensively investigated for imaging human neoplasms characterized by GRPR overexpression.

In 2020, Gu et al. [136] developed a novel GRPR-targeting peptide called GB-6. This BBN7-14-based peptide was designed to enhance metabolic stability *in vivo* and decrease intestinal uptake, while largely maintaining the original GRPR binding affinity of BBN7-14. GB-6 peptide was radiolabeled with ^{99m}Tc or conjugated with a fluorescent dye for CRC imaging. The GRPR binding properties were examined *in vitro* using Caco-2 cells [137], and the *in vivo* targeting capabilities and kinetics were assessed using Caco-2 tumor xenograft mouse models.

Additionally, comparative BBN7-14 conjugations were conducted in cellular and murine models. The GB-6 peptide demonstrates specific GRPR binding *in vitro*, exhibiting a high affinity comparable to BBN7-14. Notably, GB-6 displayed enhanced tumor uptake and reduced intestinal activity compared to the unmodified BBN7-14 probe in Caco-2 tumor-bearing mice. Experimental findings indicate that GB-6 shows promise for early detection in CRC patients and may serve as a valuable non-invasive tool for monitoring colorectal tumor progression.

HCC represents one of the most prevalent malignancies with limited diagnostic options [138-140]. The mesenchymal-epithelial transition factor (c-Met) has been found to be overexpressed in HCC, emerging as a prominent target for tumor diagnosis and treatment [141].

In 2021, Gu et al. [142] (Fig. 13B) developed a novel c-Met targeting peptide, YQ-M3, labeled with NIR fluorescent dye MPA and radionuclide ^{99m}Tc for HCC detection. YQ-M3-MPA demonstrated a high affinity for c-Met-positive HepG2 tumors *in vitro*. Fluorescence imaging revealed that YQ-M3-MPA exhibited superior tumor uptake and a higher T/N ratio in HepG2 tumor-bearing mice compared to GE137-MPA, a known c-Met-positive tracer. Furthermore, *in vivo* SPECT imaging with ^{99m}Tc-HYNIC-YQ-M3 displayed significant tumor uptake, confirming its effective localization in c-Met-positive tumor. These resultsvalidate the efficacy of YQ-M3-MPA and ^{99m}Tc-HYNIC-YQ-M3 in detecting c-Met-express-

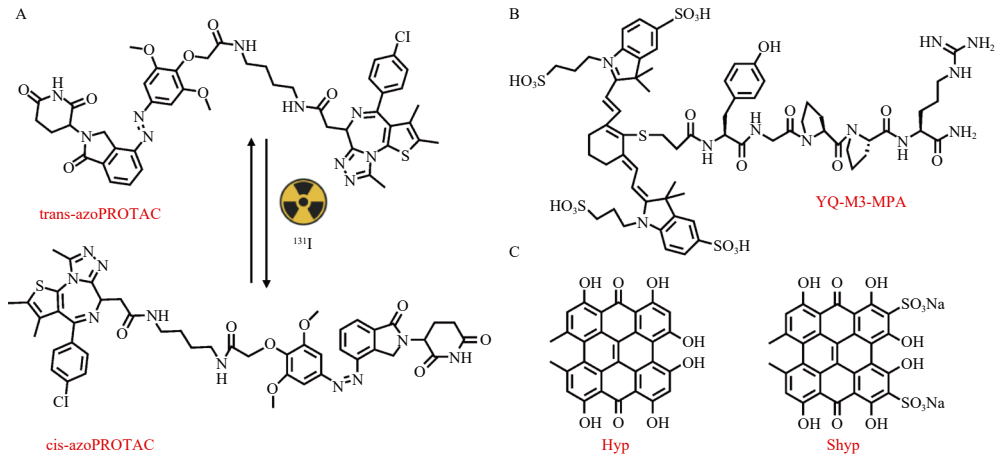

Fig. 13 Several methods for specifically enhancing the uptake of radiopharmaceuticals. (A) ^{131}I triggered photoisomerization of trans- and cis-azoPROTAC; (B) The structures of YQ-M3-MPA (C) The structures of Hyp and Shyp.

ing HCC [143].

Pancreatic cancer, specifically pancreatic ductal adenocarcinoma, ranks among the most lethal gastrointestinal malignancies, with a meager 5-year survival rate of 10.8% [144]. Despite significant medical advancements, patient outcomes for pancreatic cancer have shown minimal improvement over recent decades. This is attributed to high mortality and recurrence rates, limited resectability, rapid metastasis, and resistance to chemotherapy [145-147]. Although surgical resection remains the most effective treatment for resectable pancreatic cancer, fewer than 20% of patients are eligible for this procedure [148].

Fluorescence-guided surgical edge detection [149-151] represents one of the most promising techniques in cancer surgery, owing to its high sensitivity, real-time visualization capability, and ability to evaluate the entire surgical margin [152]. NIR fluorescent probes, including antibody-based agents targeting tumor-associated embryonic antigens, vascular endothelial growth factors, and EGFRs, have been engineered for enhanced tumor specificity. These molecular imaging agents have been investigated in both preclinical and early-phase clinical studies and have demonstrated promising utility in intraoperative fluorescence-guided imaging for the detection of pancreatic cancer [153, 154]. However, the large size of antibodies presents challenges, including slow pharmacokinetics, poor tissue penetration, neonatal Fc receptor-mediated recirculation, and enhanced permeability and retention effects, which significantly delay the time between administration of antibody-fluorophore conjugates and imaging [36, 155, 156].

Furthermore, a significant drawback of using antibody-fluorophore conjugates is their high non-specific tissue accumulation, which can lead to false-positive signals. In contrast, fluorescent probes derived from peptides, combining properties of antibodies and small molecules, offer several advantages. These include high affinity, rapid metabolism, strong tissue penetration, low immunogenicity, and ease of modification. These characteristics make peptide-based probes promising tools for cancer molecular imaging. Consequently, the discovery and development of peptide imaging agents for pancreatic cancer detection hold great significance in advancing diagnostic capabilities.

In 2023, Gu et al. [157] investigated the targeting of overexpressed GRPR in pancreatic cancer. They utilized NIR fluorescent dye MPA and radionuclide technetium-(^{99m}Tc) as targeting probes to demonstrate the efficacy of the novel peptide GB-6. The study identified a short linear peptide with enhanced *in vivo* stability. Its radiotracer [^{99m}Tc] Tc-HYNIC-PEG4-GB-6 and NIR probe MPA-PEG4-GB-6 exhibited selective and specific uptake by tumors in SW1990 pancreatic cancer xenograft mouse models. The favorable biological distribution of tracer [^{99m}Tc] TcHYNIC-PEG4-GB-6 *in vivo* led to tumor-specific accumulation 1 hour post-injection, with high tumor-muscle and bone contrast and renal body clearance. Biodistribution analysis [75, 158] revealed that the fluorescence signal ratio of SW1990 subcutaneous [159] xenograft model tumor to pancreas and intestine was 5.2 ± 0.3 and 6.3 ± 1.5, respectively. Furthermore, in orthotopic pancreatic and hepatic metastatic tumor models, the imaging probes demonstrated robust fluorescence signal accumulation within tumor tissues. Quantitative analysis revealed tumor-to-pancreas and tumor-to-liver fluorescence intensity ratios of 7.66 ± 0.48 and 3.94 ± 0.47, respectively. These high tumor-to-background contrast levels enabled precise tumor delineation. The rapid tumor targeting, precise tumor boundary delineation, chemical diversity, and high efficiency of the novel GB-6 peptide render it a high-contrast imaging probe for clinical detection of GRPR [160-162], with additional potential in molecular targeted therapy.

The development and metastasis of tumors are intricately connected to the tumor microenvironment (TME) [163-166], which encompasses cancer-associated fibroblasts (CAFs) [167], immune cells, vascular endothelial cells, and other cellular components. CAFs constitute a significant portion of the tumor stroma in most epithelial cancers. Fibroblast activation protein (FAP), a membrane-bound serine protease belonging to the dipeptidyl peptidase 4 (DPP4) family, is highly expressed in CAFs across various tumor types but is seldom detected in healthy adult tissues [168].

In numerous tumor types, the overexpression of FAP in CAFs facilitates highly selective targeting strategies utilizing FAP inhibitors (FAPI). Radionuclide-labeled quinoline FAPI has been extensively employed in tumor-targeted nuclear medicine imaging [169, 170]. However, the brief residence time of FAPI at the tumor site restricts its application in RNT [171].

In 2023, Guo et al. [172] (Fig. 14) developed a novel dimeric form of FAPI-04, which was radiolabeled with the therapeutic radionuclide ^{177}Lu for application in RNT. The dimerization strategy significantly enhanced the intratumoral retention of FAPI-04, thereby improving its performance for both diagnostic imaging and targeted radiotherapy of FAP-expressing tumors. The FAPI-04 dimer DOTA-Suc-Lys-(FAPI-04)2 was synthesized by coupling two FAPI-04 structures using Fmoc-Lys(Boc)-OH as a linker through an amide reaction. The resulting product was further functionalized with a DOTA group to enable coupling with radioactive metals. Both ^{68}Ga-(FAPI-04)2 and ^{177}Lu-(FAPI-04)2 demonstrated radiochemical purities exceeding 99% and remained stable *in vitro*. *In vivo* microscopic PET imaging of SKOV3, A431, and H1299 xenografts revealed that tumor uptake of ^{68}Ga-(FAPI-04)2 was approximately twofold higher than that of ^{68}Ga-FAPI-04. Notably, 3 hours post-injection, the accumulation of Ga-(FAPI-04)2 at the tumor site remained largely unchanged. The ^{68}Ga-(FAPI-04)2 images exhibited a significantly higher tumor-to-abdomen ratio compared to ^{18}F-FDG images. In RNT applications, ^{177}Lu (FAPI-04)2 effectively delayed tumor growth and demonstrated good tolerability.

In summary, the DOTA-Suc-Lys-(FAPI-04)2 design enhanced uptake in FAP-expressing tumors, improved residence time at tumor sites, and produced high-contrast imaging in xenografts after radionuclide labeling [173]. Furthermore, it demonstrated a significant anti-tumor effect. DOTA-Suc-Lys-(FAPI-04)2 presents a novel approach to the application of FAPI derivatives in tumor therapy.

Necrotic myocardial imaging [174-176] provides crucial indicators of the salvaged myocardial region in patients with myocardial infarction [177-179] (MI) and offers guidance for clinical decision-making [180]. A significant challenge in necrosis imaging, however, is the absence of an ideal necrosis imaging tracer capable of accurately and promptly delineating necrotic myocardium. I-131-hypericin (I-131-HYP) represents a promising tracer for precise delineation of necrotic myocardium [181]. Nevertheless, due to its high lipophilicity, clear imaging of necrotic myocardium is not achievable until 9 hours post-injection, owing to elevated background signals in the blood and lungs.

Yin et al. [180, 182] (Fig. 13C) developed an optimized ^{131}I-hypericin-2,5-disulfonate sodium salt (I-131-SHYP) probe to enhance the pharmacokinetic and biodistribution properties for necrosis imaging. The study explored the mechanism of necrotic affinity between I-131-HYP and I-131-SHYP. I-131-SHYP demonstrated selective high accumulation in necrotic cells and tissues. Biodistribution analysis revealed reduced uptake of I-131-SHYP in normal organs (lungs, spleen, and heart) and blood, as evidenced by pharmacokinetic studies [183-185].

I-131-SHYP demonstrated superior imaging of necrotic myocardium at 4 hours compared to I-131-HYP, with enhanced speed and clarity. This suggests that the increased hydrophilicity of I-131-SHYP may contribute to improved pharmacokinetic and biodistribution properties. Furthermore, DNA competitive binding assays and blocking assays indicate that E-DNA is a potential target for the necrotic affinity of SHYP and HYP. I-131-SHYP shows promise as a potential E-DNA targeting probe for necrotic myocardial imaging with molecular specificity, which may have

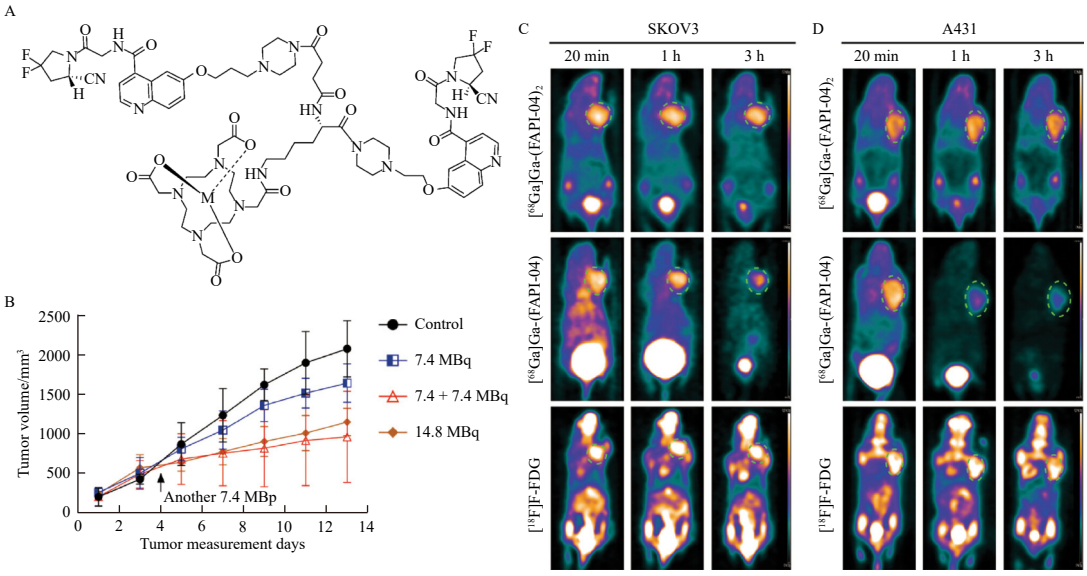

Fig. 14 The dimeric form of FAPI-04 significantly enhances its retention within tumors. (A) Synthesis and radiolabeling of DOTA-Suc-Lys-(FAPI-04)$_2$ (M = ^{68}Ga or ^{177}Lu). (B) Blood clearance curves of ^{68}Ga-FAPI-04 and ^{68}Ga-(FAPI-04)$_2$ (B) ^{177}Lu-FAPI-04, and ^{177}Lu-(FAPI-04)$_2$. (C-D) mice injected with ^{68}Ga-(FAPI-04)$_2$(3.7 MBq/0.1 mL; scale bar, 0–7%ID/g), ^{68}Ga-FAPI-04 (3.7 MBq/0.1 mL; scale bar, 0–2.5%ID/g), and ^{18}F-FDG (3.7 MBq/0.1 mL; scale bar, 0–7%ID/g) at 20 min, 1 h, and 3 h

clinical applications.

6. Prospects for the research of radionuclide drugs

Radiopharmaceuticals in medicine offer significant advantages but face numerous challenges. These include high production costs, complex regulatory approval processes, safe disposal of radioactive waste, limited supply of radionuclides with ideal half-lives, potential side effects from radiation exposure, and the requirement for specialized equipment and personnel. Furthermore, tumor cell heterogeneity and the ongoing exploration of new targets and indications present additional obstacles in the current RPT. These factors collectively restrict the widespread use of radiopharmaceuticals and motivate the medical community to seek innovative solutions to enhance their efficacy and safety. The integration of molecular biology and nanotechnology is expected to improve the targeting capabilities of radiopharmaceuticals. By attaching specific biomolecules, drugs can be delivered precisely to lesion sites, minimizing damage to healthy tissues [186]. Advancements in nuclear physics, accelerator technology, and medical reactor construction will provide cleaner nuclide sources for radiopharmaceutical research and development. Clinical data from various radionuclide drugs targeting SSTR2, PSMA, and FAP have demonstrated good tolerability and feasibility, highlighting the significant potential of radiopharmaceuticals in cancer treatment [187, 188]. The development of radionuclides with integrated diagnostic and therapeutic functions is crucial for estimating medium doses [189, 190], personalizing treatment plans, and enabling precision drug use in radionuclide drug research and development. As precision medicine advances, the application of radionuclide drugs will become increasingly personalized, with treatment plans tailored to individual genomic information, disease characteristics, and lifestyle factors. In conclusion, the future development of radionuclide drugs is expected to yield safer, more effective, and smarter solutions, making substantial contributions to human health.

Funding

The authors are grateful to the National Key R&D Program of China (No. 2023YFE0197700) and the Fundamental Research Funds for the Central Universities (No. 2632023TD04).

Declaration of competing interest

The authors declare that they have no known competing financial interests or personal relationships that could have appeared to influence the work reported in this paper.

References

1 Torre LA, Bray F, Siegel RL, et al. Global cancer statistics, 2012. *CA Cancer J Clin*. 2015;65(2):87-108. https://doi.org/10.3322/caac.21262.
2 Goldsmith S. Targeted radionuclide therapy: a historical and personal review. *Semin Nucl Med*. 2020;50(1):87-97. https://doi.org/10.1053/j.semnuclmed.2019.07.006.
3 Costa I, Cheng J, Osytek K, et al. Methods and techniques for *in vitro* subcellular localization of radiopharmaceuticals and radionuclides. *Nucl Med Biol*. 2021;98-99:18-29. https://doi.org/10.1016/j.nucmedbio.2021.03.010.
4 Wang Y, Li Y, Liu X, et al. Marine antibody-drug conjugates: design strategies and research progress. *Mar Drugs*. 2017;15(1):18. https://doi.org/10.3390/md15010018.
5 Yang S, Han G, Chen Q, et al. Au-pt nanoparticle formulation as a radiosensitizer for radiotherapy with dual effects. *Int J Nanomed*. 2021;16:239-248. https://doi.org/10.2147/IJN.S287523.
6 Goel M, Mackeyev Y, Krishnan S. Radiolabeled nanomaterial for cancer diagnostics and therapeutics: principles and concepts. *Cancer Nanotechnol*. 2023;14(1):15. https://doi.org/10.1186/s12645-023-00165-y.
7 Yang B, Kuai F, Chen Z, et al. Mir-634 decreases the radioresistance of human breast cancer cells by targeting stat3. *Cancer Biother Radiopharm*. 2020;35(3):241-248. https://doi.org/10.1089/cbr.2019.3220.
8 Salih S, Alkathieri A, Alomaim W, et al. Radiopharmaceutical treatments for cancer therapy, radionuclides characteristics, applications, and challenges. *Molecules*. 2022;27(16):5231. https://doi.org/10.3390/molecules27165231.
9 St James S, Bednarz B, Benedict S, et al. Current status of radiopharmaceutical therapy. *Int J Radiat Oncol Biol Phys*. 2021;109(4):891-901. https://doi.org/10.1016/j.ijrobp.2020.08.035.
10 Wang Z, Hu N, Li X, et al. Selection and characterization of fd164, a high-affinity signal regulatory protein α variant with balanced safety and effectiveness, from a targeted epitope mammalian cell-displayed antibody library. *Mol Pharmacol*. 2021;100(3):193-202. https://doi.org/10.1124/molpharm.120.000202.
11 Ni Q, Lu K, Pan C, et al. The treatment for a patient with cancer of unknown primary: a case report. *Dose-Response*. 2021;19(4):15593258211056185. https://doi.org/10.1177/15593258211056185.
12 Zhou J, Wang J, Chen C, et al. Usp7: target validation and drug discovery for cancer therapy. *Med Chem*. 2018;14(1):3-18. https://doi.org/10.2174/1573406413666171020115539.
13 Xia D, Zhang X, Hao H, et al. Strategies to prolong drug retention in solid tumors by aggregating Endo-CMC nanoparticles. *J Control Release*. 2023;360:705-717. https://doi.org/10.1016/j.jconrel.2023.07.006.
14 Larson S, Carrasquillo J, Cheung N, et al. Radioimmunotherapy of human tumours. *Nat Rev Cancer*. 2015;15(6):347-360. https://doi.org/10.1038/nrc3925.
15 Wang Z, Shen W, Li X, et al. The ppary agonist rosiglitazone enhances the radiosensitivity of human pancreatic cancer cells. *Drug Des Devel Ther*.

2020;14:3099-3110. https://doi.org/10.2147/DDDT.S242557.
16 Pomme S, Marouli M, Suliman G, et al. Measurement of the ^{225}Ac half-life. *Appl Radiat Isot*. 2012;70(11):2608-2614. https://doi.org/10.1016/j.apradiso.2012.07.014.
17 Zhu Y, Yin W, Yu P, et al. Meso-Hannokinol inhibits breast cancer bone metastasis *via* the ros/jnk/zeb1 axis. *Phytother Res*. 2023;37(6):2262-2279. https://doi.org/10.1002/ptr.7732.
18 Gemini-Pierini S, Ricci-Junior E, Ilem-Ozdemir D, et al. Nano-hydroxyapatite radiolabeled with radium dichloride ^{223}Ra-RaCl$_2$ for bone cancer targeted alpha therapy: *in vitro* assay and radiation effect on the nanostructure. *Colloids Surf B Biointerfaces*. 2023;223:113174. https://doi.org/10.1016/j.colsurfb.2023.113174.
19 Diniz Filho J, De Barros A, Pijera M, et al. Ultrastructural analysis of cancer cells treated with the radiopharmaceutical radium dichloride (^{223}Ra-RaCl$_2$): understanding the effect on cell structure. *Cells*. 2023;12(3):1093.
20 Lian Y, Zhu M, Yang B, et al. Characterization of a novel polysaccharide from red ginseng and its ameliorative effect on oxidative stress injury in myocardial ischemia. *Chin Med*. 2022;17(1):111. https://doi.org/10.1186/s13020-022-00669-6.
21 Wang N, Shao L, Lu W, et al. 5-Aminosalicylic acid pH-sensitive core-shell nanoparticles targeting ulcerative colitis. *J Drug Deliv Sci Technol*. 2022;74:103578. https://doi.org/10.1016/j.jddst.2022.103578.
22 Zhu B, Ren C, Du K, et al. Olean-28, 13b-olide 2 plays a role in cisplatin-mediated apoptosis and reverses cisplatin resistance in human lung cancer through multiple signaling pathways. *Biochem Pharmacol*. 2019;170:113642. https://doi.org/10.1016/j.bcp.2019.113642.
23 Filippi L, Basile P, Schillaci O, et al. The relationship between total lesion activity on ^{18}F choline positron emission tomography-computed tomography and clinical outcome in patients with castration-resistant prostate cancer bone metastases treated with ^{223}radium. *Cancer Biother Radiopharm*. 2020;35(6):398-403.
24 Xu Y, Xu J, Zhu W, et al. Bioassay-guided fractionation and biological activity of cardenolides from streptocaulon juventas. *Planta Med*. 2023;89(15):1444-1456. https://doi.org/10.1055/a-2114-5371.
25 Abbasi A, Dadashpour M, Alipourfard I. Calculation of radium-223 and actinium-225 α-emitter radiopharmaceuticals dose rates in treatment of metastatic castration-resistant prostate cancer. *J Cancer Res Ther*. 2021;17(2):348-352. https://doi.org/10.4103/jcrt.JCRT_892_18.
26 Xiao C, Li J, Kong L, et al. New cyclic c-geranylflavanones isolated from paulownia fortunei fruits with their anti-proliferative effects on three cancer cell lines. *Fitoterapia*. 2023;168:105542. https://doi.org/10.1016/j.fitote.2023.105542.
27 Hago S, Lu T, Alzain A, et al. Phytochemical constituents, *in-vitro* anticancer activity and computational studies of cymbopogon schoenanthus. *Nat Prod Res*. 2024;38(6):1073-1079. https://doi.org/10.1080/14786419.2023.2208360.
28 Abou D, Fears A, Summer L, et al. Improved ^{223}Ra therapy with combination epithelial sodium channel blockade. *J Nucl Med*. 2021;62(12):1751-1758. https://doi.org/10.2967/jnumed.121.261977.
29 Bai Z, Liu X, Guan Q, et al. 5-(3,4,5-trimethoxybenzoyl)-4-methyl-2-(p-tolyl) imidazol (bzml) targets tubulin and dna to induce anticancer activity and overcome multidrug resistance in colorectal cancer cells. *Chem Biol Interact*. 2020;315:108886. https://doi.org/10.1016/j.cbi.2019.108886.
30 Cai B, Hu Z, Tang H, et al. Triptolide impairs genome integrity by directly blocking the enzymatic activity of dna-pkcs in human cells. *Biomed Pharmacother*. 2020;129:110427. https://doi.org/10.1016/j.biopha.2020.110427.
31 Wang J, Yuan W, Shen Q, et al. The key role of organic anion transporter 3 in the drug-drug interaction between tranilast and methotrexate. *J Biochem Mol Toxicol*. 2022;36(4):e22983. https://doi.org/10.1002/jbt.22983.
32 Wei M, Su J, Ma Q, et al. Erteng tongbi decoction ameliorates collagen-induced arthritis in mice *via* modulating T cell differentiation and cytokines balance. *J Ethnopharmacol*. 2022;286:114928. https://doi.org/10.1016/j.jep.2021.114928.
33 Zhuang Y, Sun Q, Jing T, et al. Contributions of intestine and liver to the absorption and disposition of fzj-003, a selective jak1 inhibitor with structure modification of filgotinib. *Eur J Pharm Sci*. 2022;175:106211. https://doi.org/10.1016/j.ejps.2022.106211.
34 Jiang S, Pan T, Yu J, et al. Thermal and wine processing enhanced clematidis radix et rhizoma ameliorate collagen ii induced rheumatoid arthritis in rats. *J Ethnopharmacol*. 2022;288:114993. https://doi.org/10.1016/j.jep.2022.114993.
35 Correa L, De Oliveira Henriques M, Rosas E, et al. Intra-articular use of radium dichloride (^{223}Ra-RaCl$_2$) showed relevant anti-inflammatory response on experimental arthritis model. *Eur J Nucl Med Mol Imaging*. 2021;49(1):336-344. https://doi.org/10.1007/s00259-021-05515-9.
36 Xu Y, Xiao Y, Luo C, et al. Blocking PD-1/PD- L1 by an adcc enhanced anti-b7-h3/pd-1 fusion protein engages immune activation and cytotoxicity. *Int Immunopharmacol*. 2020;84:106584. https://doi.org/10.1016/j.intimp.2020.106584.
37 Fang W, Su D, Lu W, et al. Application and future prospect of extracellular matrix targeted nano-materials in tumor theranostics. *Curr Drug Targets*. 2021;22(8):913-921. https://doi.org/10.2174/1389450122666210127100430.
38 Cao Y, Cheng Y, Ihsan A, et al. A nanoparticle-coupled t2 peptide induces immune tolerance and ameliorates chronic prostatitis/chronic pelvic pain syndrome (CP/CPPS) in mice model. *Fundam Clin Pharmacol*. 2019;33(3):267-276. https://doi.org/10.1111/fcp.12438.
39 Akhmetova D, Mitusova K, Postovalova A, et al. Size-dependent therapeutic efficiency of ^{223}Ra-labeled calcium carbonate carriers for internal radionuclide therapy of breast cancer. *Biomater Sci*. 2024;12(2):453-467. https://doi.org/10.1039/D3BM01651J.
40 Sakmar M, Kozempel J, Kucka J, et al. Biodistribution study of ^{211}Pb progeny released from intravenously applied ^{223}Ra labelled tio2 nanoparticles in a mouse model. *Nucl Med Biol*. 2024;130-131:108890. https://doi.org/10.1016/j.nucmedbio.2024.108890.
41 Faulkner S, Long N. Radiopharmaceuticals for imaging and therapy. *Dalton Trans*. 2011;40(23):6067. https://doi.org/10.1039/c1dt90067f.
42 Banerjee S, Minn I, Kumar V, et al. Preclinical evaluation of $^{203/211}$Pb-labeled low-molecular-weight compounds for targeted radiopharmaceutical therapy of prostate cancer. *J Nucl Med*. 2020;61(1):80-88. https://doi.org/10.2967/jnumed.119.229393.
43 Zhu J, Li F, Gong W, et al. Long non-coding ribonucleic acid disrupted in renal carcinoma 3 inhibits chemo-resistance of prostate cancer *via* microrna-24-3p/kit ligand axis. *Indian J Pharm Sci*. 2022;84:152-161.
44 Li J, Huang T, Hua J, et al. Cd46 targeted ^{212}Pb alpha particle radioimmunotherapy for prostate cancer treatment. *J Exp Clin Cancer Res*. 2023;42(1):61. https://doi.org/10.1186/s13046-023-02636-x.
45 Jiao R, Allen K, Malo M, et al. A theranostic approach to imaging and treating melanoma with ^{203}Pb/^{212}Pb-labeled antibody targeting melanin. *Cancers*. 2023;15(15):3856. https://doi.org/10.3390/cancers15153856.
46 Kasten B, Oliver P, Kim H, et al. ^{212}Pb-labeled antibody 225.28 targeted to chondroitin sulfate proteoglycan 4 for triple-negative breast cancer therapy in mouse models. *Int J Mol Sci*. 2018;19(4):925. https://doi.org/10.3390/ijms19040925.
47 Mi S, Liu X, Zhang L, et al. Chinese medicine formula Baipuhuang Keli inhibits triple-negative breast cancer by hindering dna damage repair *via* mapk/erk pathway. *J Ethnopharmacol*. 2023;304:116077. https://doi.org/10.1016/j.jep.2022.116077.
48 Li Y, Chu Y, Shi G, et al. A novel inhibitor of arfl and arv7 induces protein degradation to overcome enzalutamide resistance in advanced prostate cancer. *Acta Pharm Sin B*. 2022;12(11):4165-4179. https://doi.org/10.1016/j.apsb.2022.05.003.
49 Poty S, Francesconi L, McDevitt M, et al. Alpha-emitters for radiotherapy: from basic radiochemistry to clinical studies-part 1. *J Nucl Med*. 2018;59(6):878-884. https://doi.org/10.2967/jnumed.116.186338.
50 Morgenstern A, Apostolidis C, Kratochwil C, et al. An overview of targeted alpha therapy with ^{225}Actinium and ^{213}Bismuth. *Curr Radiopharm*. 2018;11(3):200-208. https://doi.org/10.2174/1874471011666180502104524.
51 Banerjee S, Lisok A, Minn I, et al. Preclinical evaluation of ^{213}Bi- and ^{225}Ac-labeled low-molecular-weight compounds for radiopharmaceutical therapy of prostate cancer. *J Nucl Med*. 2021;62(7):980-988. https://doi.org/10.2967/jnumed.120.256388.
52 Liu Y, Li Y, Xu P, et al. Development of abiraterone acetate nanocrystal tablets to enhance oral bioavailability: formulation optimization, characterization, *in vitro* dissolution and pharmacokinetic evaluation. *Pharmaceutics*. 2022;14(6):1134. https://doi.org/10.3390/pharmaceutics14061134.
53 Zeng Q, Liu J, Wu Q, et al. Long non-coding RNA ac008972.1 as a novel therapeutic target for prostate cancer. *Cancer Biother Radiopharm*. 2022;39(4):291-305
54 Wharton L, Yang H, Jaraquemada-Pelaez M, et al. Rearmed bifunctional chelating ligand for ^{225}Ac/^{155}Tb precision-guided theranostic radiopharmaceuticals horizontal line h(4)noneunpaX. *J Med Chem*. 2023;66(19):13705-13730. https://doi.org/10.1021/acs.jmedchem.3c01151.
55 Li Z, Benabdallah N, Luo J, et al. Isit-qa: *in silico* imaging trial to evaluate a low-count quantitative spect method across multiple scanner-collimator configurations for ^{223}Ra-based radiopharmaceutical therapies. *J Nucl Med*. 2024;65(5):810-817. https://doi.org/10.2967/jnumed.123.266719.
56 Bokhari T, Butt M, Hina S, et al. A review on ^{90}Y-labeled compounds and biomolecules. *J Radioanal Nucl Chem*. 2017;314(3):1487-1496. https://doi.org/10.1007/s10967-017-5622-2.
57 Rong W, Wan N, Zheng X, et al. Chrysin inhibits hepatocellular carcinoma progression through suppressing programmed death ligand 1 expression. *Phytomedicine*. 2022;95:153867. https://doi.org/10.1016/j.phymed.2021.153867.
58 Zhang W, Han B, Gao C, et al. Integrated platform of oxygen self-enriched nanovesicles: sp94 peptide-directed chemo/sonodynamic therapy for liver cancer. *Eur J Pharm Biopharm*. 2022;179:206-220. https://doi.org/10.1016/j.ejpb.2022.09.012.
59 Dhondt E, Lambert B, Hermie L, et al. ^{90}Y radioembolization versus drug-eluting bead chemoembolization for unresectable hepatocellular carcinoma: results from the trace phase ii randomized controlled trial. *Radiology*. 2022;303(3):699-710. https://doi.org/10.1148/radiol.211806.
60 Primrose J. Surgery for colorectal liver metastases. *Br J Cancer*. 2010;102(9):1313-1318. https://doi.org/10.1038/sj.bjc.6605659.
61 Costa G, Spencer B, Omidvari N, et al. Radioembolization dosimetry with total-body ^{90}Y PET. *J Nucl Med*. 2022;63(7):1101-1107. https://doi.org/10.2967/jnumed.121.263145.
62 Richetta E, Pasquino M, Poli M, et al. PET-CT post therapy dosimetry in radioembolization with resin ^{90}Y microspheres: comparison with pre-treatment spect-ct ^{99m}Tc-maa results. *Phys Med Biol*. 2019;64:16-23. https://doi.org/10.1016/j.ejmp.2019.05.025.
63 Mee S, Polan D, Dewaraja Y, et al. Stereotactic body radiation therapy (SBRT) following yttrium-90 (^{90}Y) selective internal radiation therapy (sirt): a feasibility planning study using ^{90}Y delivered dose. *Phys Med Biol*. 2023;68(6):065003. https://doi.org/10.1088/1361-6560/acbbb5.
64 Dietrich A, Andreeff M, Koi L, et al. Radiotherapy enhances uptake and efficacy of ^{90}Y -cetuximab: a preclinical trial. *Radiother Oncol*. 2021;155:285-292. https://doi.org/10.1016/j.radonc.2020.11.013.
65 Yan T, Wang H, Song X, et al. Fabrication of apigenin nanoparticles using antisolvent crystallization technology: a comparison of supercritical antisolvent, ultrasonic-assisted liquid antisolvent, and high-pressure homogenization technologies. *Int J Pharm*. 2022;624:121981. https://doi.

org/10.1016/j.ijpharm.2022.121981.
66 He Y, Zhang W, Xiao Q, et al. Liposomes and liposome-like nanoparticles: from anti-fungal infection to the COVID-19 pandemic treatment. *Asian J Pharm Sci*. 2022;17(6):817-837.
67 Winter G, Hamp-Goldstein C, Fischer G, et al. Optimization of radiolabeling of a [^{90}Y]Y-anti-CD66-antibody for radioimmunotherapy before allogeneic hematopoietic cell transplantation. *Cancers*. 2023;15(14):3660. https://doi.org/10.3390/cancers15143660.
68 Budzyńska A, Kubik A, Kasperski K, et al. PET/CT and SPECT/CT imaging of ^{90}Y hepatic radioembolization at therapeutic and diagnostic activity levels: anthropomorphic phantom study. *PLoS One*. 2024;19(2):e0271711. https://doi.org/10.1371/journal.pone.0271711.
69 Ladrière T, Faudemer J, Levigoureux E, et al. Safety and therapeutic optimization of Lutetium-177 based radiopharmaceuticals. *Pharmaceutics*. 2023;15(4):1240. https://doi.org/10.3390/pharmaceutics15041240.
70 Lubberink M, Wilking H, Ost A, et al. *In vivo* instability of ^{177}Lu-dotatate during peptide receptor radionuclide therapy. *J Nucl Med*. 2020;61(9):1337-1340. https://doi.org/10.2967/jnumed.119.237818.
71 Ihsan A, Khan F, Khongorzul P, et al. Role of oxidative stress in pathology of chronic prostatitis/chronic pelvic pain syndrome and male infertility and antioxidants function in ameliorating oxidative stress. *Biomed Pharmacother*. 2018;106:714-723. https://doi.org/10.1016/j.biopha.2018.06.139.
72 Chen Y, Huang M, Zhu J, et al. Identification of a dna damage response and repair-related gene-pair signature for prognosis stratification analysis in hepatocellular carcinoma. *Front Pharmacol*. 2022;13:857060. https://doi.org/10.3389/fphar.2022.857060.
73 Ha S, O JH, Park C, et al. Dosimetric analysis of a phase I study of PSMA-targeting radiopharmaceutical therapy with [^{177}Lu]ludotatide in patients with metastatic castration-resistant prostate cancer. *Korean J Radiol*. 2024;25(2):179-188. https://doi.org/10.3348/kjr.2023.0656.
74 Banerjee S, Kumar V, Lisok A, et al. ^{177}Lu-labeled low-molecular-weight agents for PSMA-targeted radiopharmaceutical therapy. *Eur J Nucl Med Mol Imaging*. 2019;46(12):2545-2557. https://doi.org/10.1007/s00259-019-04434-0.
75 Zou J, He J, Wang X, et al. Glycoprotein ib-regulated micro platelet ghost for biosafe distribution and photothermal oncotherapy. *J Control Release*. 2022;351:341-360. https://doi.org/10.1016/j.jconrel.2022.09.036.
76 Li M, Chen H, Peng D, et al. Fu-coating pH-sensitive liposomes for improving the release of gemcitabine by endosome escape in pancreatic cancer cells. *J Drug Deliv Sci Technol*. 2023;80:104135. https://doi.org/10.1016/j.jddst.2022.104135.
77 Zhou M, Wu Y, Sun M, et al. Spatiotemporally sequential delivery of biomimetic liposomes potentiates glioma chemotherapy. *J Control Release*. 2024;365:876-888. https://doi.org/10.1016/j.jconrel.2023.11.046.
78 Zheng Z, Peng D, Li M, et al. Gemcitabine and pin1 sirna co-delivery with fucoidan-coated nano-liposomes for therapy of pancreatic cancer. *J Drug Deliv Sci Technol*. 2023;87:104872. https://doi.org/10.1016/j.jddst.2023.104872.
79 Cvjetinovic D, Prijovic Z, Jankovic D, et al. Bioevaluation of glucose-modified liposomes as a potential drug delivery system for cancer treatment using 177-Lu radiotracking. *J Control Release*. 2021;332:301-311. https://doi.org/10.1016/j.jconrel.2021.03.006.
80 Hughes J, Parsons J. Flash radiotherapy: current knowledge and future insights using proton-beam therapy. *Int J Mol Sci*. 2020;21(18):6492. https://doi.org/10.3390/ijms21186492.
81 Lamba M, Goswami A, Bandyopadhyay A. A periodic development of BPA and BSH based derivatives in boron neutron capture therapy (BNCT). *Chem Commun*. 2021;57(7):827-839. https://doi.org/10.1039/D0CC06557A.
82 Morris P, Reiner A, Szenberg O, et al. Leptomeningeal metastasis from non-small cell lung cancer survival and the impact of whole brain radiotherapy. *J Thorac Oncol*. 2012;7(2):382-385. https://doi.org/10.1097/JTO.0b013e3182398e4f.
83 Le Rhun E, Taillibert S, Zairi F, et al. A retrospective case series of 103 consecutive patients with leptomeningeal metastasis and breast cancer. *J Neurooncol*. 2013;113(1):83-92. https://doi.org/10.1007/s11060-013-1092-8.
84 Barney C, Brown A, Grosshans D, et al. Technique, outcomes, and acute toxicities in adults treated with proton beam craniospinal irradiation. *Neurooncology*. 2014;16(2):303-309.
85 Kamada T, Tsujii H, Blakely E, et al. Carbon ion radiotherapy in Japan: an assessment of 20 years of clinical experience. *Lancet Oncol*. 2015;16(2):e93-e100. https://doi.org/10.1016/S1470-2045(14)70412-7.
86 Jäkel O, Karger C, Debus J. The future of heavy ion radiotherapy. *Med Phys*. 2008;35(12):5653-5663. https://doi.org/10.1118/1.3002307.
87 Abousaida B, Seneviratne D, Hoppe B, et al. Carbon ion radiotherapy in the management of hepatocellular carcinoma. *J Hepatocell Carcinoma*. 2021;8:1169-1179. https://doi.org/10.2147/JHC.S292516.
88 Yang J, Wijetunga N, Pentsova E, et al. Randomized phase II trial of proton craniospinal irradiation versus photon involved-field radiotherapy for patients with solid tumor leptomeningeal metastasis. *J Clin Oncol*. 2022;40(33):3858. https://doi.org/10.1200/JCO.22.01148.
89 Wang Q, Xin X, Dai Q, et al. Medulloblastoma targeted therapy: from signaling pathways heterogeneity and current treatment dilemma to the recent advances in development of therapeutic strategies. *Pharmacol Ther*. 2023;250:108527. https://doi.org/10.1016/j.pharmthera.2023.108527.
90 Tran P, Pham T, Lee H, et al. Magnetic resonance imaging of pancreatic islets using tissue-adhesive particles containing iron oxide nanoparticles. *J Control Release*. 2023;364:37-45. https://doi.org/10.1016/j.jconrel.2023.10.008.
91 Simone C, Rengan R. The use of proton therapy in the treatment of lung cancers. *Cancer J*. 2014;20(6):427-432. https://doi.org/10.1097/PPO.0000000000000080.
92 Schild S, Rule W, Ashman J, et al. Proton beam therapy for locally advanced lung cancer: a review. *World J Clin Oncol*. 2014;5(4):568-575. https://doi.org/10.5306/wjco.v5.i4.568.
93 Du X, Liu W, Chen K, et al. Impact of the gastric acid suppressant use on the safety and effectiveness of egfr-tkis: a systematic review and meta-analysis. *Front Pharmacol*. 2022;13:796538. https://doi.org/10.3389/fphar.2022.796538.
94 Cao H, Zhou W, Xian X, et al. A mixture of baicalein, wogonin, and oroxylin-a inhibits emt in the A549 cell line *via* the pi3k/akt-twist1-glycolysis pathway. *Front Pharmacol*. 2022;12:821485. https://doi.org/10.3389/fphar.2021.821485.
95 Rui M, Wang Z, Fei Z, et al. The relationship between short-term surrogate endpoint indicators and mPFS and mOS in clinical trials of malignant tumors: a case study of approved molecular targeted drugs for non-small-cell lung cancer in China. *Front Pharmacol*. 2022;13:862640. https://doi.org/10.3389/fphar.2022.862640.
96 Keole S, Ashman JB, Daniels TB. Proton therapy for sarcomas. *Cancer J*. 2014;20(6):409-414. https://doi.org/10.1097/PPO.0000000000000084.
97 Pugh TJ, Lee AK. Proton beam therapy for the treatment of prostate cancer. *Cancer J*. 2014;20(6):415-420. https://doi.org/10.1097/PPO.0000000000000083.
98 Cheng P, Wu J, Zong G, et al. Capsaicin shapes gut microbiota and pre-metastatic niche to facilitate cancer metastasis to liver. *Pharmacol Res*. 2023;188:106643. https://doi.org/10.1016/j.phrs.2022.106643.
99 Kuok C, Wang Q, Fong P, et al. Inhibitory effect of hernandezine on the proliferation of hepatocellular carcinoma. *Biol Pharm Bull*. 2023;46(2):245-256. https://doi.org/10.1248/bpb.b22-00612.
100 Jiang L, Li L, Liu Y, et al. Drug resistance mechanism of kinase inhibitors in the treatment of hepatocellular carcinoma. *Front Pharmacol*. 2023;14:1097277. https://doi.org/10.3389/fphar.2023.1097277.
101 Malouff TD, Peterson JL, Mahajan A, et al. Carbon ion radiotherapy in the treatment of gliomas: a review. *J Neurooncol*. 2019;145(2):191-199. https://doi.org/10.1007/s11060-019-03303-y.
102 Combs SE, Kessel K, Habermehl D, et al. Proton and carbon ion radiotherapy for primary brain tumors and tumors of the skull base. *Acta Oncol*. 2013;52(7):1504-1509. https://doi.org/10.3109/0284186X.2013.818255.
103 Barth RF, Coderre JA, Vicente MG, et al. Boron neutron capture therapy of cancer: current status and future prospects. *Clin Cancer Res*. 2005;11(11):3987-4002. https://doi.org/10.1158/1078-0432.CCR-05-0035.
104 Luderer MJ, De La Puente P, Azab AK. Advancements in tumor targeting strategies for boron neutron capture therapy. *Pharm Res*. 2015;32(9):2824-2836. https://doi.org/10.1007/s11095-015-1718-y.
105 Xu H, Liu J, Li R, et al. Novel promising boron agents for boron neutron capture therapy: current status and outlook on the future. *Coord Chem Rev*. 2024;511:215795. https://doi.org/10.1016/j.ccr.2024.215795.
106 Kueffer PJ, Maitz CA, Khan AA, et al. Boron neutron capture therapy demonstrated in mice bearing EMT6 tumors following selective delivery of boron by rationally designed liposomes. *Proc Natl Acad Sci U S A*. 2013;110(16):6512-6517. https://doi.org/10.1073/pnas.1303437110.
107 Milkereit R, Persaud A, Vanoaica L, et al. LAPTM4b recruits the LAT1-4F2hc Leu transporter to lysosomes and promotes mTORC1 activation. *Nat Commun*. 2015;6:7250. https://doi.org/10.1038/ncomms8250.
108 Michiue H, Sakurai Y, Kondo N, et al. The acceleration of boron neutron capture therapy using multi-linked mercaptoundecahydrododecaborate (BSH) fused cell-penetrating peptide. *Biomaterials*. 2014;35(10):3396-3405. https://doi.org/10.1016/j.biomaterials.2013.12.055.
109 Li R, Zhang J, Guo J, et al. Application of nitroimidazole-carbobane-modified phenylalanine derivatives as dual-target boron carriers in boron neutron capture therapy. *Mol Pharm*. 2020;17(1):202-211. https://doi.org/10.1021/acs.molpharmaceut.9b00898.
110 Chen L, Zhang X, Cao Q, et al. Development and application of a physiologically based pharmacokinetic model for HPPH in rats and extrapolate to humans. *Eur J Pharm Sci*. 2019;129:68-78. https://doi.org/10.1016/j.ejps.2018.12.014.
111 Zhou TJ, Xing L, Fan YT, et al. Light triggered oxygen-affording engines for repeated hypoxia-resistant photodynamic therapy. *J Control Release*. 2019;307:44-54. https://doi.org/10.1016/j.jconrel.2019.06.016.
112 Zhou TJ, Xing L, Fan YT, et al. Inhibition of breast cancer proliferation and metastasis by strengthening host immunity with a prolonged oxygen-generating phototherapy hydrogel. *J Control Release*. 2019;309:82-93. https://doi.org/10.1016/j.jconrel.2019.07.028.
113 Fan W, Huang P, Chen X. Overcoming the Achilles' heel of photodynamic therapy. *Chem Soc Rev*. 2016;45(23):6488-6519. https://doi.org/10.1039/C6CS00616G.
114 Shaffer TM, Pratt EC, Grimm J. Utilizing the power of Cerenkov light with nanotechnology. *Nat Nanotechnol*. 2017;12(2):106-117. https://doi.org/10.1038/nnano.2016.301.
115 Wang Q, Liu N, Hou Z, et al. Radioiodinated persistent luminescence nanoplatform for radiation-induced photodynamic therapy and radiotherapy. *Adv Healthc Mater*. 2021;10(5):e2000802. https://doi.org/10.1002/adhm.202000802.
116 Li Z, Zhang Y, Wu X, et al. Direct aqueous-phase synthesis of sub-10 nm"Luminous Pearls"with enhanced *in vivo* renewable near-infrared persistent luminescence. *J Am Chem Soc*. 2015;137(16):5304-5307. https://doi.org/10.1021/jacs.5b00872.
117 Baig M MFA, Naveed M, Abbas M, et al. DNA scaffold nanoparticles coated with HPMC/EC for oral delivery. *Int J Pharm*. 2019;562:321-32. https://doi.org/10.1016/j.ijpharm.2019.03.054.
118 Huang L, Asghar S, Zhu T, et al. Advances in chlorin-based photodynamic therapy with nanoparticle delivery system for cancer treatment. *Expert*

Opin Drug Deliv. 2021;18(10):1473-1499. https://doi.org/10.1080/17425247.2021.1950685.
119 Xu Y, Yao Y, Wang L, et al. Hyaluronic acid coated liposomes co-delivery of natural cyclic peptide RA-XII and mitochondrial targeted photosensitizer for highly selective precise combined treatment of colon cancer. *Int J Nanomed*. 2021;16:4929-4942. https://doi.org/10.2147/IJN.S311577.
120 Kamkew A, Cheng L, Goel S, et al. Cerenkov radiation induced photodynamic therapy using chlorin e6-loaded hollow mesoporous silica nanoparticles. *ACS Appl Mater Interfaces*. 2016;8(40):26630-26637. https://doi.org/10.1021/acsami.6b10255.
121 Guo J, Feng K, Wu W, et al. Smart ^{131}I-labeled self-illuminating photosensitizers for deep tumor therapy. *Angew Chem Int Ed Engl*. 2021;60(40):21884-21889. https://doi.org/10.1002/anie.202107231.
122 Li J, Zhang J, Yang S, et al. Synthesis and preclinical evaluation of radioiodinated hypericin dicarboxylic acid as a necrosis avid agent in rat models of induced hepatic, muscular, and myocardial necroses. *Mol Pharm*. 2016;13(1):232-240. https://doi.org/10.1021/acs.molpharmaceut.5b00686.
123 Liu N, Shi Y, Guo J, et al. Radioiodinated tyrosine based carbon dots with efficient renal clearance for single photon emission computed tomography of tumor. *Nano Res*. 2019;12(12):3037-3043. https://doi.org/10.1007/s12274-019-2549-7.
124 Sun Y, Zhao D, Wang G, et al. Recent progress of hypoxia-modulated multifunctional nanomedicines to enhance photodynamic therapy: opportunities, challenges, and future development. *Acta Pharm Sin B*. 2020;10(8):1382-1396. https://doi.org/10.1016/j.apsb.2020.01.004.
125 Gao HL, Xiao D, Gong GY, et al. Vielanin P enhances the cytotoxicity of doxorubicin *via* the inhibition of PI3K/Nrf2-stimulated MRP1 expression in MCF-7 and K562 DOX-resistant cell lines. *Phytomedicine*. 2019;58:152885. https://doi.org/10.1016/j.phymed.2019.152885.
126 Qin SY, Zhang AQ, Zhang XZ. Recent advances in targeted tumor chemotherapy based on smart nanomedicines. *Small*. 2018;14(45):e1802417. https://doi.org/10.1002/smll.201802417.
127 Velema WA, Szymanski W, Feringa BL. Photopharmacology: beyond proof of principle. *J Am Chem Soc*. 2014;136(6):2178-2191. https://doi.org/10.1021/ja413063e.
128 Liu H, Wang Q, Guo J, et al. Prodrug-based strategy with a two-in-one liposome for Cerenkov-induced photodynamic therapy and chemotherapy. *J Control Release*. 2023;364:206-215. https://doi.org/10.1016/j.jconrel.2023.10.036.
129 Shi Q, Tong Y, Zheng Y, et al. PDT-sensitized ROS-responsive dextran nanosystem for maximizing antitumor potency of multi-target drugs. *Int J Pharm*. 2023;633:122567. https://doi.org/10.1016/j.ijpharm.2022.122567.
130 Li Z, Shen Y, Wang Y, et al. Perfluorocarbon nanoemulsions for combined pulmonary siRNA treatment of lung metastatic osteosarcoma. *Adv Ther*. 2019;2(7):1900039. https://doi.org/10.1002/adtp.201900039.
131 Yu L, Wang Y, He Y, et al. Combination of apatinib with apo-IDO1 inhibitor for the treatment of colorectal cancer. *Int Immunopharmacol*. 2022;112:109233. https://doi.org/10.1016/j.intimp.2022.109233.
132 Yun X, Zhang Q, Fang Y, et al. Madecassic acid alleviates colitis-associated colorectal cancer by blocking the recruitment of myeloid-derived suppressor cells *via* the inhibition of IL-17 expression in γδT17 cells. *Biochem Pharmacol*. 2022;202:115138. https://doi.org/10.1016/j.bcp.2022.115138.
133 Yu W, Huang J, Dong Q, et al. Ag120-mediated inhibition of ASCT2-dependent glutamine transport has an anti-tumor effect on colorectal cancer cells. *Front Pharmacol*. 2022;13:871392. https://doi.org/10.3389/fphar.2022.871392.
134 Morgat C, MacGrogan G, Brouste V, et al. Expression of gastrin-releasing peptide receptor in breast cancer and its association with pathologic, biologic, and clinical parameters: a study of 1 432 primary tumors. *J Nucl Med*. 2017;58(9):1401-1407. https://doi.org/10.2967/jnumed.116.188011.
135 Fleischmann A, Waser B, Gebbers JO, et al. Gastrin-releasing peptide receptors in normal and neoplastic human uterus: involvement of multiple tissue compartments. *J Clin Endocrinol Metab*. 2005;90(8):4722-4729. https://doi.org/10.1210/jc.2005-0964.
136 Liu P, Tu Y, Tao J, et al. GRPR-targeted SPECT imaging using a novel bombesin-based peptide for colorectal cancer detection. *Biomater Sci*. 2020;8(23):6764-6772. https://doi.org/10.1039/D0BM01432J.
137 Yang Y, Ren R, Chen Q, et al. *Coptis chinensis* polysaccharides dynamically influence the paracellular absorption pathway in the small intestine by modulating the intestinal mucosal immunity microenvironment. *Phytomedicine*. 2022;104:154322. https://doi.org/10.1016/j.phymed.2022.154322.
138 Ayuso C, Rimola J, Vilana R, et al. Diagnosis and staging of hepatocellular carcinoma (HCC): current guidelines. *Eur J Radiol*. 2018;101:72-81. https://doi.org/10.1016/j.ejrad.2018.01.025.
139 Gong QZ, Xiao D, Gong GY, et al. EH-42: a novel small molecule induces apoptosis and inhibits migration and invasion of human hepatoma cells through suppressing STAT3 signaling pathway. *Curr Cancer Drug Targets*. 2019;19(7):583-593. https://doi.org/10.2174/1568009619666181226094814.
140 Sun J, Tao R, Mao T, et al. The involvement of lipid raft pathway in suppression of TGFβ-mediated metastasis by tolfenamic acid in hepatocellular carcinoma cells. *Toxicol Appl Pharmacol*. 2019;380:114696. https://doi.org/10.1016/j.taap.2019.114696.
141 Wang H, Rao B, Lou J, et al. The function of the HGF/c-Met axis in hepatocellular carcinoma. *Front Cell Dev Biol*. 2020;8:55. https://doi.org/10.3389/fcell.2020.00055.
142 Tang Y, Xu H, Dai Y, et al. A novel peptide targeting c-Met for hepatocellular carcinoma diagnosis. *J Mater Chem B*. 2021;9(22):4577-4586. https://doi.org/10.1039/D1TB00408E.
143 Yang Y, Liao Y, Gui YP, et al. GL-V9 reverses adriamycin resistance in hepatocellular carcinoma cells by affecting JNK2-related autophagy. *Chin J Nat Med*. 2020;18(7):491-499.
144 Siegel RL, Miller KD, Fuchs HE, et al. Cancer statistics, 2021. *CA Cancer J Clin*. 2021;71(1):7-33. https://doi.org/10.3322/caac.21654.
145 Zeng SL, Li SZ, Lai CJS, et al. Evaluation of anti-lipase activity and bioactive flavonoids in the Citri Reticulatae Pericarpium from different harvest time. *Phytomedicine*. 2018;43:103-109. https://doi.org/10.1016/j.phymed.2018.04.008.
146 Baig M MFA, Khan S, Naeem MA, et al. Vildagliptin loaded triangular DNA nanospheres coated with eudragit for oral delivery and better glycemic control in type 2 diabetes mellitus. *Biomed Pharmacother*. 2018;97:1250-1258.
147 Khan GJ, Rizwan M, Abbas M, et al. Pharmacological effects and potential therapeutic targets of DT-13. *Biomed Pharmacother*. 2018;97:255-263.
148 Kamisawa T, Wood LD, Itoi T, et al. Pancreatic cancer. *Lancet*. 2016;388(10039):73-85. https://doi.org/10.1016/S0140-6736(16)00141-0.
149 Xue X, Li Q, Zhang P, et al. PET/NIR fluorescence bimodal imaging for targeted tumor detection. *Mol Pharm*. 2023;20(12):6262-6271. https://doi.org/10.1021/acs.molpharmaceut.3c00660.
150 Zhang L, Wang B, Yin G, et al. Rapid fluorescence sensor guided detection of urinary tract bacterial infections. *Int J Nanomed*. 2022;17:3723-3733. https://doi.org/10.2147/IJN.S377575.
151 Li R, Shu M, Tian Y, et al. Quantum dots combined with a fluorescence-linked immunosorbent assay for detecting the metabolic balance of DT-13 excretion in rats. *J Pharm Biomed Anal*. 2020;190:113508. https://doi.org/10.1016/j.jpba.2020.113508.
152 Fujita K, Kamiya M, YoshioKA T, et al. Rapid and accurate visualization of breast tumors with a fluorescent probe targeting alpha-mannosidase 2C1. *ACS Cent Sci*. 2020;6(12):2217-2227. https://doi.org/10.1021/acscentsci.0c01189.
153 De Valk KS, Deeken MM, Schaap DP, et al. Dose-finding study of a CEA-targeting agent, SGM-101, for intraoperative fluorescence imaging of colorectal cancer. *Ann Surg Oncol*. 2021;28(3):1832-1844. https://doi.org/10.1245/s10434-020-09069-2.
154 Sun X, Liu L, Zou H, et al. Intelligent drug delivery microparticles with visual stimuli-responsive structural color changes. *Int J Nanomed*. 2020;15:4959-4967. https://doi.org/10.2147/IJN.S249009.
155 Tummers WS, Miller SE, Teraphongphom NT, et al. Intraoperative pancreatic cancer detection using tumor-specific multimodality molecular imaging. *Ann Surg Oncol*. 2018;25(7):1880-1888. https://doi.org/10.1245/s10434-018-6453-2.
156 Gao Y, Zeng Y, Xue W, et al. Anti-IL-12/23 p40 antibody attenuates chronic graft-versus-host disease with lupus nephritis *via* inhibiting Tfh cell in mice. *Biomed Pharmacother*. 2020;129:110396.
157 Tu Y, Han Z, Pan R, et al. Novel GRPR-targeting peptide for pancreatic cancer molecular imaging in orthotopic and liver metastasis mouse models. *Anal Chem*. 2023;95(30):11429-11439. https://doi.org/10.1021/acs.analchem.3c01765.
158 Dai X, Zhao W, Tong X, et al. Non-clinical immunogenicity, biodistribution and toxicology evaluation of a chimpanzee adenovirus-based COVID-19 vaccine in rat and rhesus macaque. *Arch Toxicol*. 2022;96(5):1437-1453. https://doi.org/10.1007/s00204-021-03221-x.
159 Zhao Z, Li M, Zheng L, et al. Noninvasive transdermal delivery of mesoporous silica nanoparticles using deep eutectic solvent. *J Control Release*. 2022;343:43-56. https://doi.org/10.1016/j.jconrel.2022.01.019.
160 Peng H, Wang J, Chen J, et al. Challenges and opportunities in delivering oral peptides and proteins. *Expert Opin Drug Deliv*. 2023;20(10):1349-1369. https://doi.org/10.1080/17425247.2023.2237408.
161 Zhang T, Luo X, Xu K, et al. Peptide-containing nanoformulations: skin barrier penetration and activity contribution. *Adv Drug Deliv Rev*. 2023;203:115139. https://doi.org/10.1016/j.addr.2023.115139.
162 Yang J, Huo Y, Jin X, et al. Compatibility study of peptide and glycerol using chromatographic and spectroscopic techniques: application to a novel antimicrobial peptide Cbf-14 gel. *Pharmaceutics*. 2023;15(12):2784. https://doi.org/10.3390/pharmaceutics15122784.
163 Zhang C, Fei Y, Wang H, et al. CAFs orchestrates tumor immune microenvironment-a new target in cancer therapy?*Front Pharmacol*. 2023;14:1113378. https://doi.org/10.3389/fphar.2023.1113378.
164 Sun X, Zhou L, Wang Y, et al. Single-cell analyses reveal cannabidiol rewires tumor microenvironment *via* inhibiting alternative activation of macrophage and synergizes with anti-PD-1 in colon cancer. *J Pharm Anal*. 2023;13(7):726-744. https://doi.org/10.1016/j.jpha.2023.04.013.
165 Li Z, Deng Y, Sun H, et al. Redox modulation with a perfluorocarbon nanoparticle to reverse Treg-mediated immunosuppression and enhance anti-tumor immunity. *J Control Release*. 2023;358:579-590. https://doi.org/10.1016/j.jconrel.2023.05.013.
166 Zhou X, Zhang P, Liu N, et al. Enhancing chemotherapy for pancreatic cancer through efficient and sustained tumor microenvironment remodeling with a fibroblast-targeted nanosystem. *J Control Release*. 2023;361:161-177. https://doi.org/10.1016/j.jconrel.2023.07.061.
167 Fu S, Song X, Hu Y, et al. Neotuberostemonine and tuberostemonine ameliorate pulmonary fibrosis through suppressing TGF-β and SDF-1 secreted by macrophages and fibroblasts *via* the PI3K-dependent AKT and ERK pathways. *Chin J Nat Med*. 2023;21(7):527-539.
168 Fitzgerald AA, Weiner LM. The role of fibroblast activation protein in health and malignancy. *Cancer Metastasis Rev*. 2020;39(3):783-803. https://doi.org/10.1007/s10555-020-09909-3.
169 Jansen K, Heirbaut L, Cheng JD, et al. Selective inhibitors of fibroblast activation protein (FAP) with a (4-quinolinoyl)-glycyl-2-cyanopyrrolidine scaffold. *ACS Med Chem Lett*. 2013;4(5):491-496. https://doi.org/10.1021/ml300410d.

170 Loktev A, Lindner T, Mier W, et al. A tumor-imaging method targeting cancer-associated fibroblasts. *J Nucl Med*. 2018;59(9):1423-1429. https://doi.org/10.2967/jnumed.118.210435.

171 Zhao L, Niu B, Fang J, et al. Synthesis, preclinical evaluation, and a pilot clinical PET imaging study of ^{68}Ga-labeled FAPI dimer. *J Nucl Med*. 2022;63(6):862-868. https://doi.org/10.2967/jnumed.121.263016.

172 Zhong X, Guo J, Han X, et al. Synthesis and preclinical evaluation of a novel FAPI-04 dimer for cancer theranostics. *Mol Pharm*. 2023;20(5):2402-2414. https://doi.org/10.1021/acs.molpharmaceut.2c00965.

173 Jiang X, Yang X, Shi Y, et al. Maackiain inhibits proliferation and promotes apoptosis of nasopharyngeal carcinoma cells by inhibiting the MAPK/Ras signaling pathway. *Chin J Nat Med*. 2023;21(3):185-196. https://doi.org/10.1016/S1875-5364(23)60420-0.

174 Mikrani R, Liang C, Naveed M, et al. A cardiac troponin I study in a minimally invasive myocardial infarction canine model. *Appl Biomed*. 2019;17(1):39. https://doi.org/10.32725/jab.2018.001.

175 Li X, He S, Liang W, et al. Marsdenia tenacissima injection induces the apoptosis of prostate cancer by regulating the AKT/GSK3β/STAT3 signaling axis. *Chin J Nat Med*. 2023;21(2):113-126. https://doi.org/10.1016/S1875-5364(23)60389-9.

176 Wu P, Zhang Z, Ma G, et al. Transcriptomics and metabolomics reveal the cardioprotective effect of Compound Danshen tablet on isoproterenol-induced myocardial injury in high-fat-diet fed mice. *J Ethnopharmacol*. 2020;246:112210. https://doi.org/10.1016/j.jep.2019.112210.

177 Lai Q, Yuan G, Wang H, et al. Metabolomic profiling of metoprolol-induced cardioprotection in a murine model of acute myocardial ischemia. *Biomed Pharmacother*. 2020;124:109820. https://doi.org/10.1016/j.biopha.2020.109820.

178 Li X, Mikrani R, Li C, et al. An epicardial delivery of nitroglycerine by active hydraulic ventricular support drug delivery system improves cardiac function in a rat model. *Drug Deliv Transl Res*. 2020;10(1):23-33. https://doi.org/10.1007/s13346-019-00656-9.

179 Liao J, Zhang Y, Ma C, et al. Microbiome-metabolome reveals that the Suxiao Jiuxin Pill attenuates acute myocardial infarction associated with fatty acid metabolism. *J Ethnopharmacol*. 2023;312:116529. https://doi.org/10.1016/j.jep.2023.116529.

180 Wang C, Jin Q, Yang S, et al. Synthesis and evaluation of ^{131}I-Skyrin as a necrosis avid agent for potential targeted radionuclide therapy of solid tumors. *Mol Pharm*. 2016;13(1):180-189. https://doi.org/10.1021/acs.molpharmaceut.5b00630.

181 Wu X, Liu L, Zheng Q, et al. Dihydrotanshinone I preconditions myocardium against ischemic injury *via* PKM2 glutathionylation sensitive to ROS. *Acta Pharm Sin B*. 2023;13(1):113-127. https://doi.org/10.1016/j.apsb.2022.07.006.

182 Duan X, Yin Z, Jiang C, et al. Radioiodinated hypericin disulfonic acid sodium salts as a DNA-binding probe for early imaging of necrotic myocardium. *Eur J Pharm Biopharm*. 2017;117:151-159. https://doi.org/10.1016/j.ejpb.2017.04.006.

183 Pei L, Li R, Zhou H, et al. A physiologically based pharmacokinetic approach to recommend an individual dose of tacrolimus in adult heart transplant recipients. *Pharmaceutics*. 2023;15(11):2580. https://doi.org/10.3390/pharmaceutics15112580.

184 Wu X, Sia JEV, Hai M, et al. Physiologically based pharmacokinetic model for older adults and its application in geriatric drug research. *Curr Drug Metab*. 2023;24(3):211-222. https://doi.org/10.2174/1389200224666230509104404.

185 Xu R, Liu W, Ge W, et al. Physiologically-based pharmacokinetic pharmacodynamic parent-metabolite model of edoxaban to predict drug-drug-disease interactions: M4 contribution. *CPT Pharmacometrics Syst Pharmacol*. 2023;12(8):1093-1106. https://doi.org/10.1002/psp4.12977.

186 Chen Q, Li Y, Zhou S, et al. Sequentially sustained release of anticarcinogens for postsurgical chemoimmunotherapy. *J Control Release*. 2022;350:803-814. https://doi.org/10.1016/j.jconrel.2022.09.006.

187 Yang L, Wang Y, Ye X, et al. Traditional Chinese medicine-based drug delivery systems for anti-tumor therapies. *Chin J Nat Med*. 2024;22(12):1177-1192. https://doi.org/10.1016/S1875-5364(24)60746-6.

188 Yin T, Wu Q, Wang L, et al. Well-defined redox-sensitive polyethene glycol-paclitaxel prodrug conjugate for tumor-specific delivery of paclitaxel using octreotide for tumor targeting. *Mol Pharm*. 2015;12(8):3020-3031. https://doi.org/10.1021/acs.molpharmaceut.5b00280.

189 Ni X, Tang X, Wang D, et al. Research progress of sensors based on molecularly imprinted polymers in analytical and biomedical analysis. *J Pharm Biomed Anal*. 2023;235:115659. https://doi.org/10.1016/j.jpba.2023.115659.

190 Jin Y, Han G, Gao Y, et al. Serum-tolerant polymeric complex for stem-cell transfection and neural differentiation. *Nat Commun*. 2025;16(1):2022. https://doi.org/10.1038/s41467-025-57278-8.